IBRACON Structures and Materials Journal
Revista IBRACON de Estruturas e Materiais
ISSN 1983-4195 ismj.org

REVIEW PAPER

Shear and punching shear according to the Critical Shear Crack Theory: background, recent developments and integration in codes

Corte e punçoamento de elementos de betão armado de acordo com a Teoria da Fissura de Corte Crítica: enquadramento histórico, desenvolvimentos recentes e integração em normas

Aurelio Muttoni[a]
João Tiago Simões[a]

[a]Ecole Polytechnique Fédérale de Lausanne, Lausanne, Switzerland

Received 24 February 2023
Accepted 24 March 2023

Abstract: The Critical Shear Crack Theory (CSCT) has been developed since 1985 to assess the shear resistance of members without shear reinforcement and the punching shear resistance of reinforced concrete slabs in a rational manner. The main idea of the CSCT is that the shear resistance is governed by the development of a critical shear crack, its geometry and its kinematics. Recent shear tests with detailed measurements have confirmed that the shear force can be carried through the critical shear crack by a combination of aggregate interlocking, residual tensile strength of concrete, dowel action of the longitudinal reinforcement, inclination of the compression zone and activation of the shear reinforcement crossed by the critical shear crack if present. On the basis of advanced constitute laws, all these contributions can be calculated as a function of the crack geometry and its kinematic. Simplifications of the resulting general formulations have been implemented in several standards including the *fib* Model Code 2010 and, in its recent closed-form format, in the second generation of the European Standard for Concrete Structures. The generality of the models allows accounting for several materials and cases, as for instance the presence of axial forces, fiber reinforced concrete, non-metallic reinforcements and designing strengthening using several techniques. This document presents the historical framework of the development of the theory, followed by a short presentation of its most up-to-date refined models. The derivation of closed-form solutions based on the CSCT and how it leads to expressions in a format similar to the current European Standard for Concrete Structures is also discussed. Eventually, for the case of punching, some recent developments are shown in what refers the capability of the refined mechanical model to capture the relationship between the acting punching load, the rotation and the shear deformation during loading and at failure.

Keywords: shear, punching shear, mechanical model, codes, levels-of-approximation.

Resumo: A Teoria da Fissura de Corte Crítica (CSCT, referindo-se à sua definição Critical Shear Crack Theory na língua Inglesa) tem sido desenvolvida desde 1985 para avaliar a resistência ao corte de elementos de betão armado sem armadura de esforço transverso assim como a resistência ao punçoamento de lajes e fundações de betão armado. A principal ideia desta teoria é a de que a resistência é condicionada pelo desenvolvimento de uma fissura de corte crítica, nomeadamente pela sua geometria e cinemática. Ensaios experimentais realizados recentemente demonstram que o esforço transverso pode ser transmitido através da fissura de corte crítica devido à soma de várias contribuições, nomeadamente: engrenamento dos agregados, resistência à tração residual do betão, efeito de ferrolho das armaduras longitudinais, contribuição da zona comprimida e activação da armadura de esforço transverso atravessada pela fissura crítica (nos casos em que esta exista). Todas estas contribuições podem ser devidamente quantificadas em função da geometria e cinemática da fissura de corte crítica, usando para o efeito relações constitutivas adequadas. Versões simplificadas das formulações mais refinadas e gerais dos modelos mecânicos da CSCT foram introduzidas em diversos documentos normativos, tais como o Código Modelo 2010 da *fib* ou, mais recentemente, a segunda geração da Norma Europeia para Estruturas de Betão Armado. A generalidade dos modelos da teoria permite utilizá-los para outros casos particulares, tais como seja a presença de esforço normal, o caso de elementos de betão com fibras, armaduras não metálicas ou o dimensionamento de soluções de reforço estrutural. Este documento apresenta um enquadramento histórico do desenvolvimento da teoria, seguido de uma apresentação muito sucinta dos seus modelos refinados mais atuais.

Corresponding author: Aurelio Muttoni. E-mail: aurelio.muttoni@epfl.ch
Financial support: None.
Conflict of interest: Nothing to declare.
Data Availability: data-sharing is not applicable to this article as no new data were created or analyzed in this study.

É ainda discutida a derivação de expressões de forma fechada baseada na CSCT, o que conduz a expressões com um formato idêntico às que constam no atual Eurocódigo 2. Finalmente, para o caso de punçoamento, alguns dos desenvolvimentos mais recentes da teoria são apresentados, nomeadamente no que se refere à capacidade do modelo refinado de relacionar a carga, a rotação e a deformação por corte, não somente na rotura mas também durante o carregamento.

Palavras-chave: corte, punçoamento, modelo mecânico, normas, níveis de aproximação.

How to cite: A. Muttoni and J. T. Simões, "Shear and punching shear according to the Critical Shear Crack Theory: background, recent developments and integration in codes," *Rev. IBRACON Estrut. Mater.*, vol. 16, no. 3, e16302, 2023, https://doi.org/10.1590/S1983-41952023000300002

1 INTRODUCTION

The need for a safe and sound design against brittle failures is a well-established design principle to ensure robust structures. Shear or punching shear are among the most known sources of brittle failures in reinforced concrete structures. In concrete slabs, a major difference between shear and punching is the principal shear force direction with respect to the support [1]. In "one-way shear" (as for instance in the slab supported on two walls with a distributed load as shown in Figure 1b), the shear principal directions are parallel between them and normally perpendicular to the linear supports. In punching shear, or "two-way shear", the shear principal directions predominantly converge to the support (or propagate from a concentrated load) in a radial manner (see red shear trajectories in Figure 1a). The shear resistance can be the governing design criterion in linear members with shear reinforcement or in planar members without shear reinforcement where linear supports are provided, such as slabs with significant distributed loads (Figure 1b), slabs with discontinuities, shells, retaining walls or slabs with concentrated loads in the vicinity of linear supports (Figure 1c). Punching shear is the common governing design criterion in flat slabs near to columns, wall ends and wall corners, or when concentrated loads are applied to planar members, such as slabs, shells and column bases.

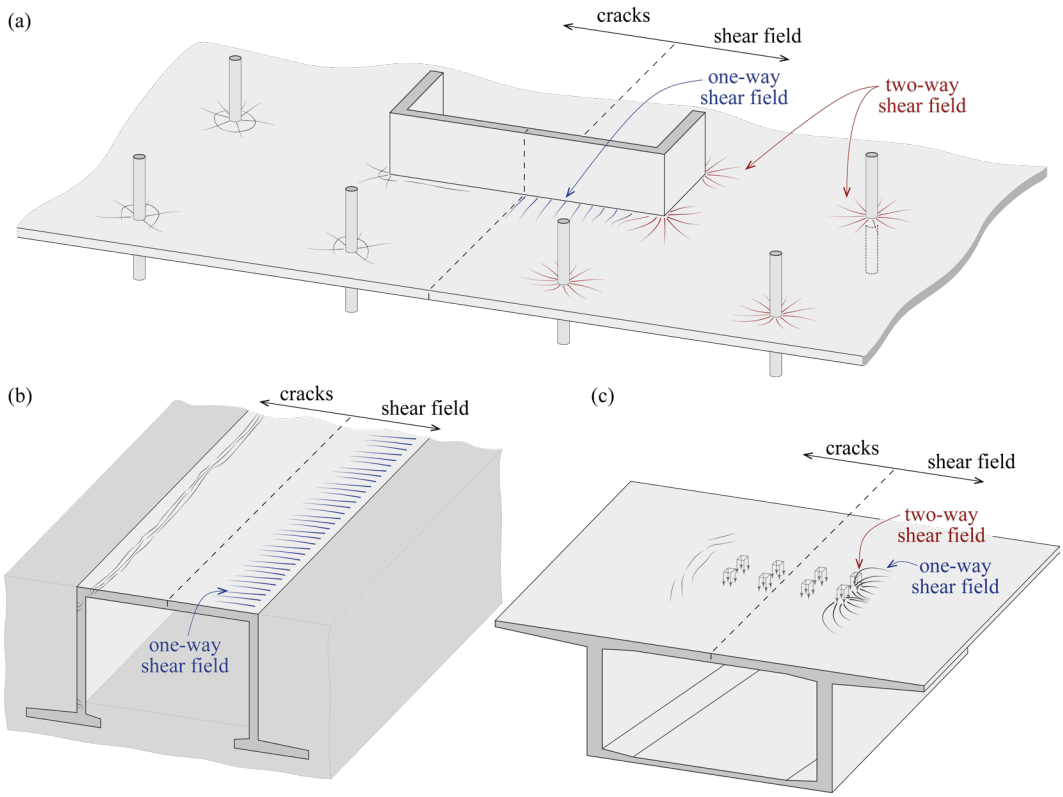

Figure 1. Examples of structural reinforced concrete members where shear or punching shear can be the governing design criterion.

Whitin the group of reinforced concrete members potentially failing in shear, a difference has to be made between members with shear reinforcement (such as beams, columns or transition walls) and members without shear reinforcement (typically slabs, shells and retaining walls). In the former case, if more than minimum shear

reinforcement is provided, the shear failure will occur by yielding of the shear reinforcement or/and crushing of concrete carrying the inclined compression field, thus being associated with a given deformation capacity (distributed cracking, see for instance [2]). On the contrary, shear failures in members without shear reinforcement take place by strain localization along a critical shear crack associated with a very limited deformation capacity [1], [3]. This fundamental difference has led to the development of different design methods for each one of the cases.

For members with shear reinforcement, two different models have been proposed and implemented in standards: (1) the so called "variable truss angle model" based on [2], [4] (implemented for instance in the European Standard for Structural Concrete 5,6]; which is in fact a compression field model where the concrete tensile strength is neglected) and (2) the approaches where the compression field contribution is combined with the contributions which can be observed in members without shear reinforcement [5] (implemented for instance in North American Standards [6]).

For members without shear reinforcement, the behavior and the failure mechanism are complex so that the design has been historically based on methods with a strong empirical basis (see for instance [7], [8] for shear in one-way members and [9]–[12] for punching shear). Mechanical considerations and mechanical models have also been proposed in the last century (see for instance [3], [13]–[19] for shear in one-way members and [20]–[23] for punching shear). Some of them were strain-based [3], [18], [20], [22], allowing to explicitly calculate the shear resistance on the basis of the deformations in the localization zone. Nevertheless, until 1993 [24], the size effect was considered in standards only on an empirical basis and mechanically based strain-based models have been implemented for the first time in a standard only in 2003 [25].

It was in this context that the Critical Shear Crack Theory (CSCT) has been proposed some decades ago to account for strain and size effect in a rational manner and allowing to implement for the first time these effects in standards [24], [25]. Since then, the theory has evolved, being nowadays well consolidated for both research and design purposes.

This keynote article presents an overview of the CSCT, starting with the background including an historical overview followed by the recent developments. It discusses not only the advances on the level of the theoretical model (with the development of refined mechanical formulations), but also its implementation in codes of practice.

2 HISTORICAL BACKGROUNDS OF THE CRITICAL SHEAR CRACK THEORY

2.1 Main ideas

The CSCT has been developed since 1985 to assess the shear resistance of members without shear reinforcement and the punching shear resistance of reinforced concrete slabs in a rational manner. The research started with a design proposal for punching [26] and an experimental work on concrete beams without shear reinforcement which has shown that the shear resistance is typically governed by the development of a Critical Shear Crack (CSC) and its kinematics [27], [28]. The CSCs typically develop starting from the tensile zone as flexural cracks, slightly inclined in presence of a shear force. For low load levels, the crack opens mainly in mode I (Figure 2) due to the elongation of the flexural reinforcement. For higher load levels, the crack becomes flatter, the center of rotation follows the tip of the crack so that the crack opens in combined mode I-II with an increasing sliding component (Figure 2).

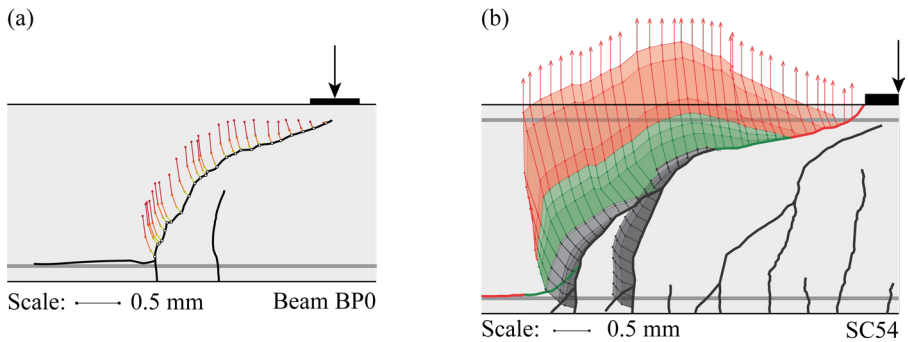

Figure 2. Research on the development of the critical shear crack and associated kinematics: (a) original measurements [27], [28] and (b) recent measurements with refined techniques [29].

The original cardboard model shown in Figures 3a has been prepared at the beginnings of the CSCT to explain the failure process in an intuitive manner: the shear resistance is reached when the opening of the CSC due to bending (Figure 3a1) reduces the capacity to carry shear stresses through the crack by aggregate interlocking. The CSC can thus

almost freely develop in the compression zone (only the activation of the dowel action in the flexural reinforcement and the residual tensile strength in the sub-horizontal branch of the CSC oppose to its development) leading finally to the shear failure (Figure 3a2).

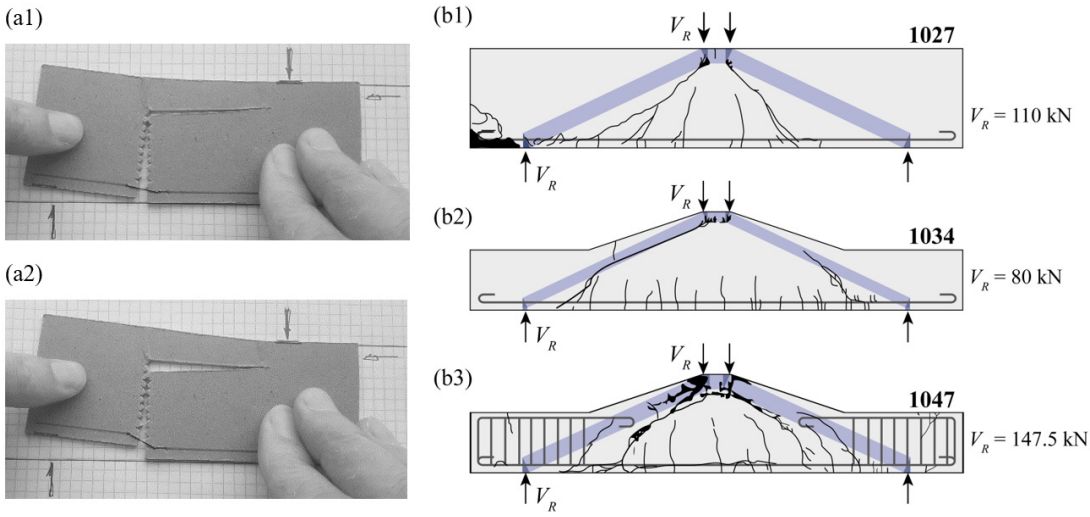

Figure 3. First conceptual ideas and experimental evidence grounding the CSCT for shear in beams and slabs without shear reinforcement: (a) original cardboard model from 1985 with (a1) flexural crack in Mode I and (a2) flexural crack in combined mode I-II; (b) figure from reference [28] presenting the experimental results by Mörsch [30], whose interpretation supports the idea that the location and shape of the CSC influences the failure load (theoretical direct struts carrying shear shown in blue).

In addition, a systematic interpretation of test results described in the literature has also shown that the location of the CSC with respect to loads and supports can have a significant influence on the shear resistance. This is mainly due to the fact that if the CSC is not located in a region where a direct strut can develop between load and support, a significant shear force can be carried without activating the aggregate interlocking across the CSC. This is shown for instance in Figure 3b from [28]: in the case of Figure 3b1, the crack developed without interaction with the theoretical direct strut due to poor bond conditions (plain bars were used) and the beam failed eventually due to insufficient anchorage at the support; in the tapered beam of Figure 3b2, the CSC developed in a unfavorable manner reducing significantly the capacity of the direct strut, leading to a strength reduction of 27% compared to previous case; on the contrary, in a very similar beam shown in Figure 3b3, the top reinforcement of the beam ends was sufficiently long to reach the theoretical strut, thus controlling the opening of the CSC, and eventually allowing for an increased shear resistance (134%). This matter of fact explains the significant influence of the load location with respect to the support (loads applied at a distance < 3d from the support) on the shear resistance [13], [14], [28], [31]–[33] and the scatter of the experimental results which can be observed in members without shear reinforcement (as a small deviation of the shape and position of the CSC can have a significant influence on the shear resistance).

2.2 Development of the mechanical model for punching shear and applications

The considerations presented above have been implemented in a mechanical model to calculate the punching shear resistance of slabs without shear reinforcement with the initial aim of quantifying the size effect in a rationally sound manner for the revision of the Swiss Code for concrete structures SIA 162 of 1993 [24]. The main ideas at that time were (see reference [32]):

- The opening in Mode I of the CSC which develops near to the column with an inclination of about 45° is proportional to the product $\psi \cdot d$, where d is the effective depth of the slab and ψ is the slab rotation outside the slab-column connection (see blue arrows in Figure 4a);
- The rotation ψ can be calculated as a function of the acting load (and thus of the shear force) assuming an elastic-plastic flexural behavior of the slab as proposed by Kinnunen and Nylander [20];

- The shear stresses which are activated in the CSC due to crack sliding (combined Mode I-II) can be estimated for the adopted kinematics with the model by Walraven [35]. Their integration provides the shear resistance which is a function of the crack opening (Mode I, and therefore of the product $\psi \cdot d$) leading to the so-called failure criterion.

The failure criterion has been calibrated on the basis of the experimental results available in the literature at that time (Figure 4b) allowing to calculate the punching shear resistance in a reliable manner on the basis of the main parameters. Figure 4c, presented in reference [32] in 1991, depicts for instance the normalized punching shear resistance as a function of the effective depth, showing clearly the size effect which depends also on the flexural reinforcement ratio (with higher detrimental size effects for slabs with higher flexural reinforcement ratios and brittler behavior). With this mechanical model, it was possible to design also tailored solutions as for instance the punching shear resistance in presence of steel shear heads where the contribution of the embedded steel structure and its influence on the deformation could be considered in a rational manner [36].

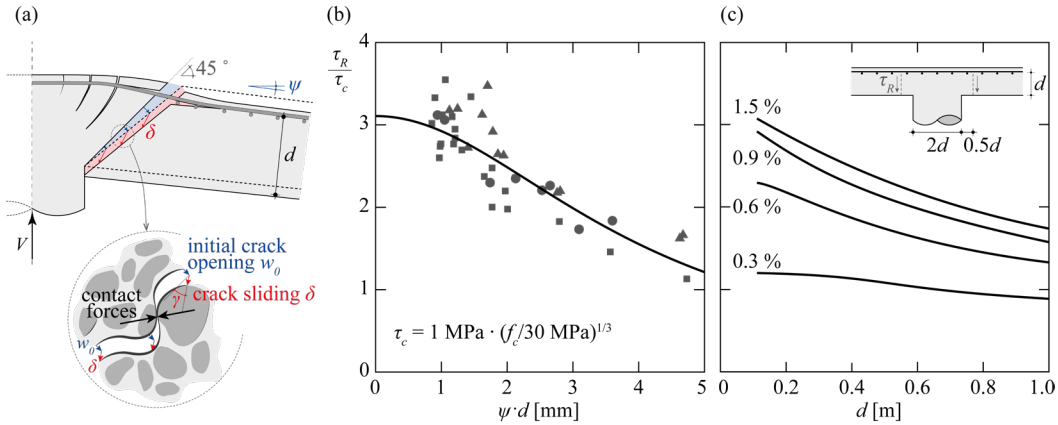

Figure 4. CSCT for punching shear between 1985 to 1991, with: (a) assumptions on the shape and kinematics of the CSC to calculate the interlocking stresses between crack lips (opening in Mode I due to flexure shown in blue, combined Mode I-II due to shear shown in red); (b) adoption of an analytical failure criterion calibrated on the basis of experimental results; (c) calculated normalized punching resistance with the proposed model for different flexural reinforcement ratios as a function of the effective depth (figures (a) adapted from [34], (b) and (c) adapted from [32]).

Since 2000, the principles of the CSCT for punching shear have been improved and applied to several situations and cases:

- Improvement of the load-rotation relationship accounting for tension stiffening and for the uncracked zones; improvement of the failure criterion accounting for the aggregate size in a physical sound manner [37]–[39];
- Experimental validation for different slabs thicknesses, columns sizes and flexural reinforcements ratios [40]–[43];
- Punching of slabs with shear reinforcement [44]–[49];
- Extension of the CSCT to steel fiber reinforced concrete [50];
- Investigation of retrofitting methods with post-installed shear reinforcement [51], [52], using externally bonded fiber reinforced polymers [53] or other techniques [54];
- Investigation of edge and corner connections, internal slab-column connections with non-symmetric reinforcement or rectangular columns [55]–[57];
- Experimental validation for different aggregate sizes, improvement of the analytical definition of the failure criterion, investigation of the effect of significant axial forces in the columns in case of multi-story buildings [58], [59];
- Experimental and theoretical investigation of post-tensioned slabs and slabs with axial forces [60]–[62];
- Internal slab-column connections with unbalanced moments, deformation capacity of flat slabs with imposed horizontal displacements, monotonic and cyclic loading [63]–[66];
- General considerations on the size effect [67];
- Experimental and theoretical investigation of foundation rafts and column bases [68]–[70];
- Experimental and theoretical investigation of the residual load-carrying capacity after punching and on the efficiency of integrity reinforcement to prevent progressive collapse [71];
- Investigation of the influence of compressive membrane actions in flat slabs and redistribution between hogging and sagging moments in continuous slabs [72], [73];

- Verification of actual slabs combining the failure criterion of the CSCT with the rotation calculated on the basis of NLFEA [74]–[81];
- Punching of slabs in case of impact loading [82], [83];
- Detailed measurements to better assess the failure process [84];
- Improvement of the mechanical model to better account for the actual failure mechanism [70], [85], see also subsection 3.2.2 below;
- Development of closed-form solutions to be implemented in standards following current Eurocode 2 format [86]–[88], see also subsection 3.2.3 below;
- Investigation of internal slab-column connections with openings [89];
- Investigation of the serviceability limit state of flat slabs on the basis of the CSCT [90];
- Investigation of the influence of corroded reinforcement on the punching shear resistance and deformation capacity of flat slabs [91];
- Investigation of lightweight aggregate concrete flat slabs with ultra-high fiber reinforced concrete in the compression zone [92].

2.3 Development of the mechanical model for shear in one-way members and applications

With respect to the shear resistance of one-way members without shear reinforcement, the opening of the CSC can be assumed to be proportional to the product of the longitudinal strain and the effective depth (further details will be given in subsection 3.1 below). Since the reinforcement is usually in the elastic range, the governing longitudinal strain can be easily calculated with a sectional analysis. The mechanical model has been presented in 2003 [37], [93] (see [33] for an English translation) and implemented in the Swiss code for concrete structures SIA 262:2003 [25]. Also in this case, based on a failure criterion calibrated on experimental results (Figure 5a), it was possible to calculate the shear resistance on the basis of the main geometrical and mechanical parameters. Figure 5b shows for instance the size effect on the shear resistance. It is interesting to note that, since the normalized shear resistance becomes smaller for deeper members, also the longitudinal reinformed required for bending becomes smaller. This means that for a member designed both for shear and bending, the combined size and strain effect (descending failure criterion in Figure 5a) leads to a more pronounced reduction of the shear resistance for deeper members (see the steeper curve in Figure 5b, see also [94] for further details).

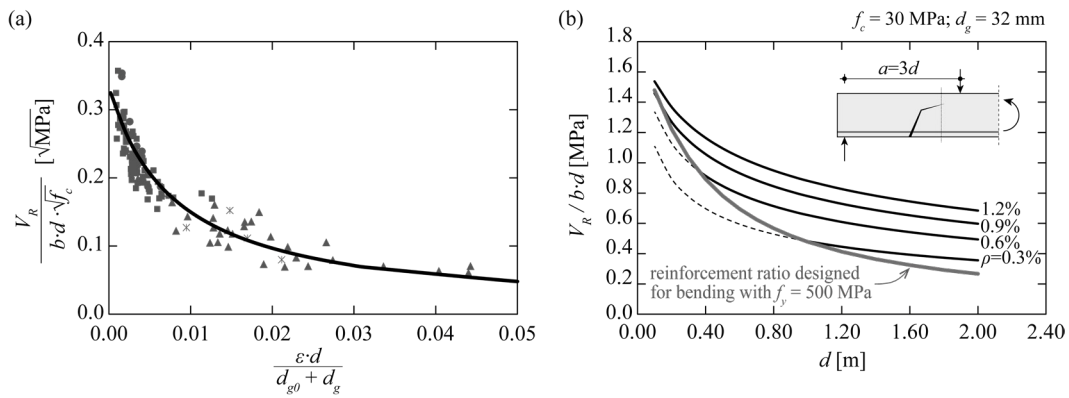

Figure 5. Critical shear crack theory for shear in one-way members between 2000 to 2003, with: (a) adoption of an analytical failure criterion calibrated on the basis of experimental results (adapted from [37], [93]); (b) calculated shear resistance varying the value of the effective depth (according to [37], [93]).

It is also interesting to mention that already in its original form [33], [37], [93], the CSCT allowed to account for the presence of an axial force (which has a direct influence on the reference longitudinal strain, see also subsection 3.1.3 below), lightweight aggregate concrete (reduced aggregate interlocking) and a non-metallic reinforcement (increased longitudinal strain due to the lower elastic modulus, and therefore reduced shear resistance).

Since 2003, the principles CSCT for shear in one-way members without shear reinforcement has been improved and applied to different situations and cases:

- Reduction of the shear resistance in case of yielding of longitudinal reinforcement and calculation of rotation capacity as a function of the shear force in members without shear reinforcement [95], [96];
- Shear force distribution in slabs with concentrated loads near linear supports [97]–[99];
- Detailed analysis of shear-transfer actions in RC members based on measured cracking pattern and failure kinematics [29], [100]–[105];
- Theoretical considerations on the shear transfer actions and implications to size effects [67], [94], [102], [106];
- Influence of distributed loads [102], [103], [107], [108];
- Shear resistance of T-beams [109], tapered [107] and curved members [110];
- Detailed quantification of the shear transfer actions and improvement of the mechanical model [102], [103], [108], see also subsections 3.1.1 and 3.1.2 below;
- Development of closed-form solutions to be implemented in standards [102], [105], [106], see also subsection 3.1.3 below;
- Influence of fatigue loading on shear failures of reinforced concrete members without shear reinforcement [111], [112];
- Development of the model for fiber reinforced concrete and low amounts of shear reinforcement [103];
- Characterization of shear deformations and implications for the shear force redistribution in slabs [113].

Most of the above-mentioned references resulted directly or indirectly from researches performed at École Polytechnique Fédérale de Lausanne, Switzerland, but a large number of other works performed by different research groups have also contributed to further validate and extend the theory (some references are already presented above, without the ambition to be exhaustive).

2.4 Implementation of the CSCT in Standards

The CSCT and its ideas have been implemented in following standards:

- Swiss code for concrete structures SIA 162:1989 [114]: punching provisions including minimum flexural resistances required to limit the rotation [26];
- CEB-FIP MC1990 [115]: implementation of the minimum flexural resistances from [26] in the punching shear provisions;
- Swiss code for concrete structures SIA 162, revision 1993 [24]: implementation of the size effect according to the CSCT [32];
- Swiss code for concrete structures SIA 262:2003 [25]: full implementation of the CSCT for shear in slabs without shear reinforcement [33], [37], [93], and for punching shear [37], [39];
- *fib* Model Code 2010 [116]: implementation of the CSCT in the punching shear provisions [117] and new provision to avoid progressive collapse of flat slabs [71];
- draft for the second generation of Eurocode 2 FprEN 1992-1-1:2023 [118]:
  - closed-form expression of the CSCT for shear in one-way slabs without shear reinforcement based on the development presented in [102], [105], [106] (further details are presented in section 3.1.3 below);
  - closed-form expression of the CSCT for punching without and with shear reinforcement based on the development presented in [34], [86], [87], [88] with further improvements according to [49] (further details are presented in section 3.2.4 below);
  - strain-based approach adapted from [33],[[37], [93] for a detailed assessment of the shear resistance of existing slabs (Annex for existing structures);
  - strain-based approach adapted from [37], [39], [117] for a detailed assessment of the punching shear resistance of existing slabs (Annex for existing structures);
  - provisions adapted from [71] to avoid progressive collapse of flat slab.

3 RECENT DEVELOPMENTS OF THE CRITICAL SHEAR CRACK THEORY

3.1 Shear in beams and slabs without shear reinforcement

3.1.1 Recent experimental evidence

The generalization of the use of Digital Image Correlation (DIC) to follow in detail the behavior of reinforced concrete members is allowing steps forward in the understanding of complex phenomena (e.g. [29], [119]). With respect to the shear response of beams and slabs without shear reinforcement, a number of relevant experimental evidence has been presented in recent years (see references [29], [101]–[103], [106] for further details):

- The DIC allows identifying and tracking quasi-continuously the development of the CSC, see Figure 6a. By dividing the actual CSC into a finite number of segments with its measured geometry and kinematics (Figure 6b), the relative contribution of the different shear-transfer actions can be calculated with advanced constitutive laws (Figure 6c). Such procedure applied to different load levels, different specimens with varying boundary and loading conditions, as well as geometrical and mechanical properties, allowed concluding that the sum of all shear-transfer actions contributing to carry shear across the critical section corresponds fairly well with the experimentally acting shear load (during loading and at failure), see Figure 6d for an example. If such a procedure was already possible with conventional techniques [100], DIC allows to conduct the measurement just before and after reaching the maximum load.
- The relative contribution of each shear-transfer action depends on the location and shape of the CSC. When the tip of the CSC is close to the load introduction, the contribution of the compression chord is higher than in the cases where the tip of the CSC is far from the load. In this latter case, shear is mainly carried by aggregate interlocking, residual tensile strength and dowel action.
- DIC also allows to investigate in a systematic manner the geometry of the CSC. As identified long ago by various researchers [18], the CSC for shear in beams and slabs without shear reinforcement can be simplified by a bi-linear shape with a stepper branch on the tension side and a flatter one close to the compression side.
- With respect to the kinematics of the CSC, the crack opening along the height of the CSC shows a linear profile if the crack opening of different secondary flexural crack (associated with bond) is summed in a tributary length.

More details can be found in reference [102] which presents a summarized overview on recent findings [29], [101], [103], [106].

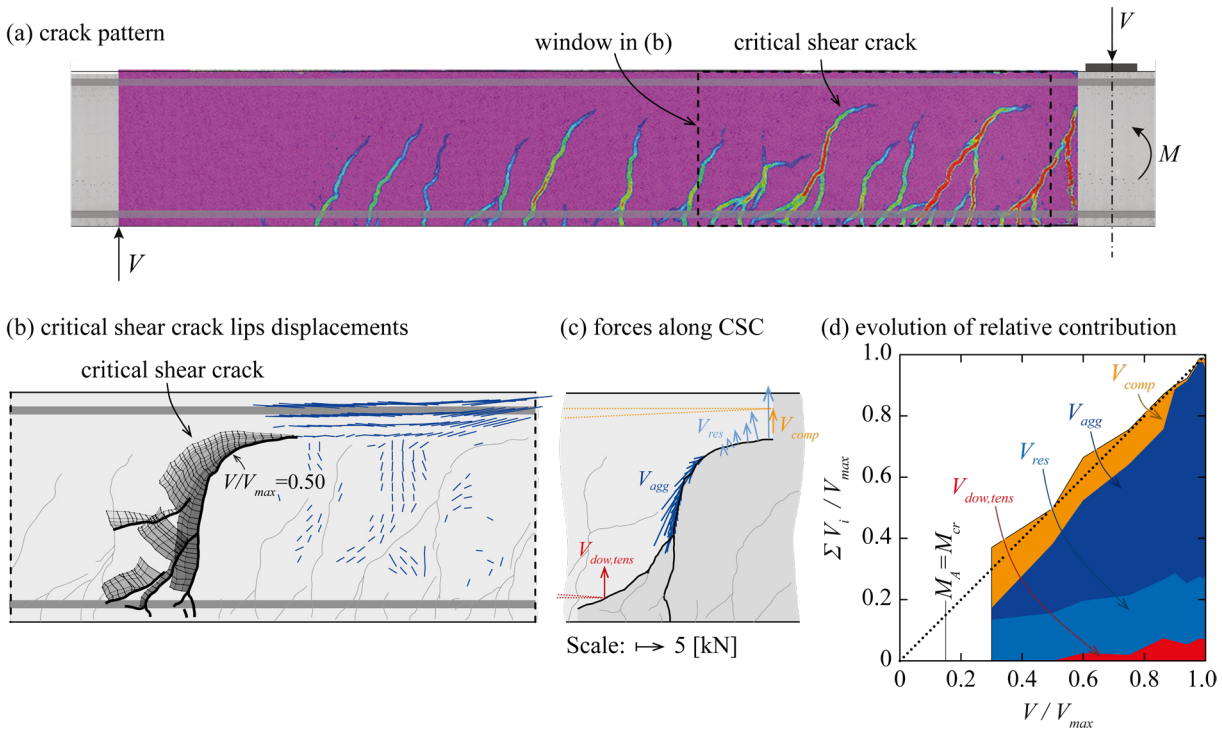

Figure 6. Application of DIC to investigate the cracking development and associated kinematics in specimen SC70 by Cavagnis et al. [101]: (a) crack pattern at V_{max}; (b) measured crack lips displacements and compressive strains in the shear critical region at V_{max}; (c) acting forces in the critical shear crack at V_{max}; (d) evolution of relative contribution of each shear-transfer action during loading. Figure adapted from [102].

3.1.2 Refined formulation of the mechanical model

Based on the principles of the CSCT (development of flexural shear cracks reducing the shear-carrying capacity), with an assumed bi-linear shape of the CSC (as already considered by [18], see Figure 7a-7b), the crack kinematics can be derived assuming the rotation between rigid bodies (Figure 7c-7e). Using advanced constitutive laws as described

by Cavagnis et al. [102], [108], all different shear transfer actions shown in Figure 7f can be calculated: aggregate interlocking V_{agg}, residual tensile strength after cracking V_{tens}, dowel action of the longitudinal reinforcement V_{dow} and shear carried by the compression zone V_{com}. The sum of all these contributions provides the failure criterion (Figure 7g) and the shear resistance for a given cross-section can be calculated intersecting the load-deformation relationship from equilibrium and stress-strain relationship of the longitudinal reinforcement.

The shear resistance of the member can be calculated for the different sections along the length of the beam (corresponding to different load-strain relationships and shapes of the CSC), eventually allowing to search for the section that yields the minimum resistance (governing section, see Figure 7h).

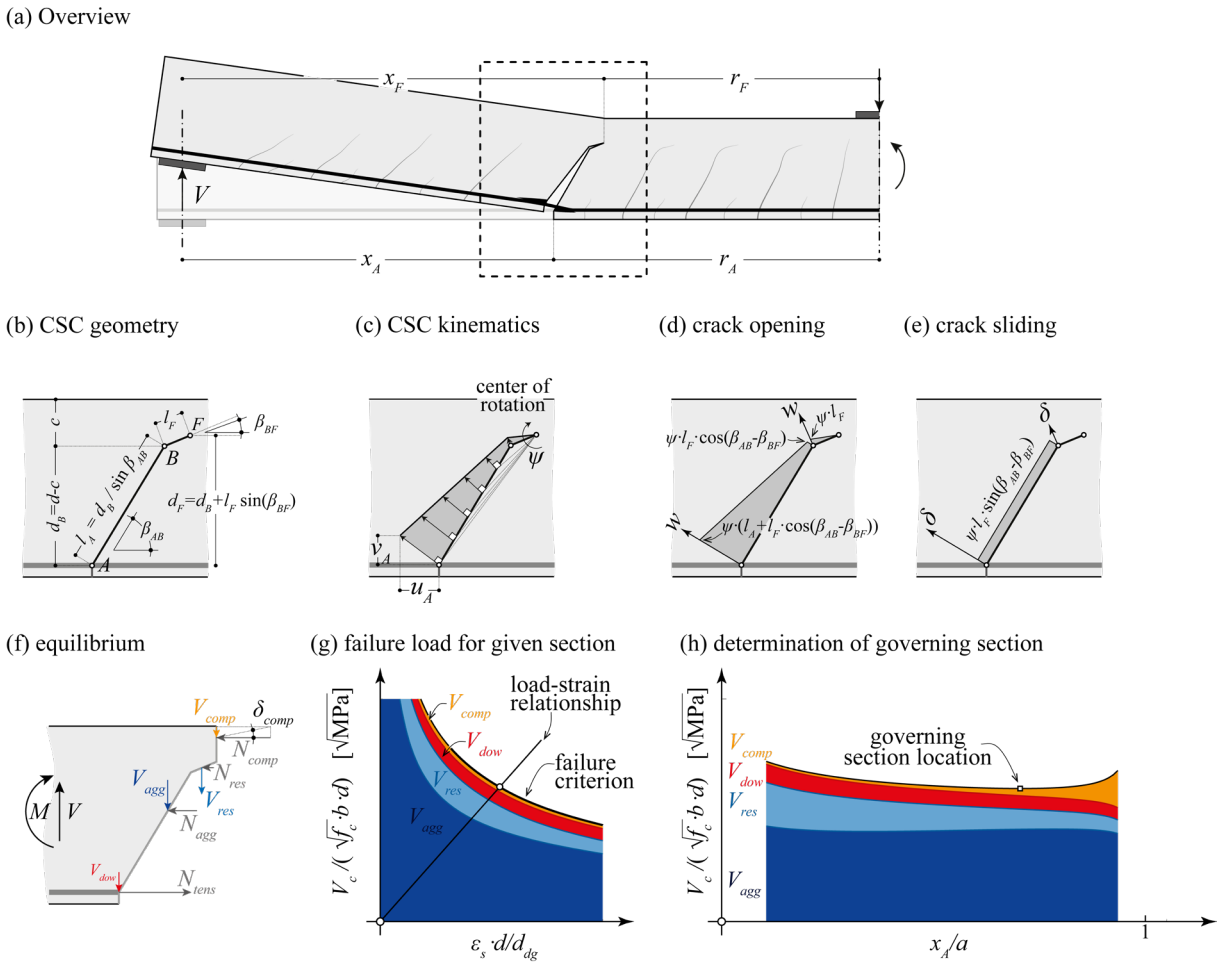

Figure 7. Mechanical model based on the development of a critical shear crack according to [102], [108]. Figure adapted from [102].

3.1.3 Closed-form expressions and Integration to codes of practice

The refinement of the mechanical model by Cavagnis et al. [102], [108] presented above can be used to establish a generalized failure criterion which describes the normalized shear resistance as a function of the normalized crack width. The latter is represented by the ratio $\varepsilon_s \cdot d/d_{dg}$ (see Figure 7g), where ε_s is the strain of the tensile flexural reinforcement and d_{dg} is the reference value of the crack roughness d_{dg} = 16 mm + $d_g \leq$ 40 mm, with d_g being the maximum aggregate size (to be reduced for high strength concretes [120]; value of d_{dg} with upper limit in accordance with [121]). Eventually, as a simplification for practical purposes (see Figure 8 and reference [102] for validation through a systematic parametric study), the analytical failure criterion (V_c) of Equation 1 can be assumed:

$$V_c = 0.015 \cdot k_c \cdot k_\beta \cdot \left(\frac{d_{dg}}{\varepsilon_s \cdot d}\right)^{\frac{1}{2}} \cdot \sqrt{f_c} \cdot b \cdot d \tag{1}$$

where f_c refers to the cylinder compressive concrete strength; b and d to the width and effective depth; k_c and k_β account respectively for the location and shape of the CSC (see reference [102] for details).

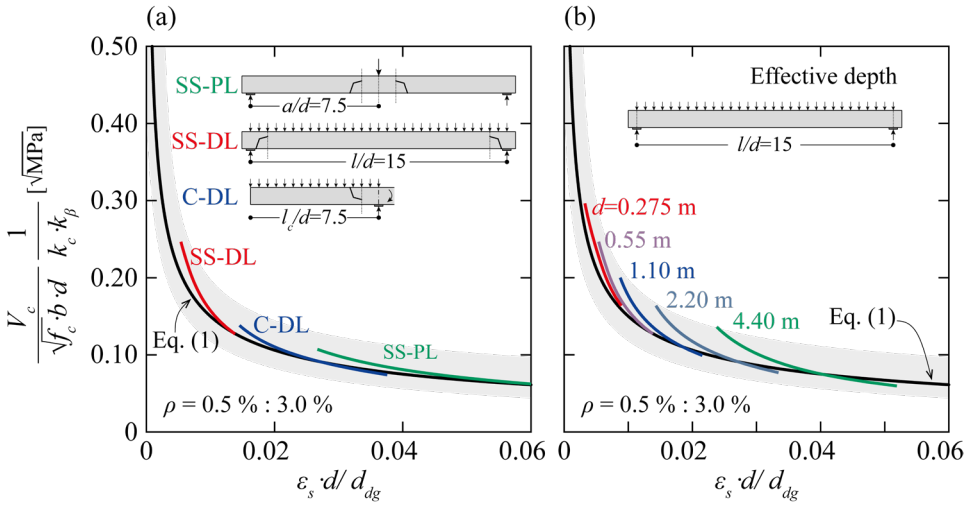

Figure 8. Failure criterion calculated with the refined formulation of the mechanical model of the CSCT obtained varying (a) ρ or (b) d and comparison with the analytical power-law failure criterion (values when not varied: d=0.55 m; f_c=40 MPa; d_g=16 mm). Figure adapted from [102].

Considering that the longitudinal reinforcement remains elastic, the load-deformation relationship can be easily derived from a sectional analysis with the bending moment $V_E \cdot a_{cs}$:

$$\varepsilon_s = \frac{V_E \cdot a_{cs}}{z \cdot \rho \cdot b \cdot d \cdot E_s} \tag{2}$$

where V_E is the acting shear load; a_{cs} is the moment-to-shear ratio at the control section; z is the lever arm; E_s is the modulus of elasticity and ρ is the flexural reinforcement ratio. A closed-form equation can then be obtained for the shear resistance as follows (considering V_E=V_c=V_R) [102]:

$$\frac{V_R}{b \cdot d} = 0.75 \cdot \left(k_c \cdot k_\beta\right)^{2/3} \cdot \left(100 \cdot \rho \cdot f_c \frac{d_{dg}}{a_{cs}}\right)^{\frac{1}{3}} \tag{3}$$

Equation 3 can be further simplified to (considering a constant value for k_c and a value for k_β as a function of a_{cs}, whose values depend on the adopted control section) [102]:

$$\frac{V_R}{b \cdot d} = 0.75 \cdot \left(100 \cdot \rho \cdot f_c \frac{d_{dg}}{\sqrt{d \cdot a_{cs}}}\right)^{\frac{1}{3}} \tag{4}$$

This expression is similar to the one in current Eurocode 2 – Concrete Structures [122] (which has completely empirical origin [8]), but accounts for the strain and size effect in a rational manner. In addition, it also acknowledges the influence of the type of concrete (by means of parameter d_{dg}) and the moment-to-shear ratio a_{cs} on the shear resistance of members without shear reinforcement. As discussed above (see also references [102] and [123]), Equation 4 has been integrated in section 8 (Ultimate Limit States) of the second generation of Eurocode 2 – Concrete Structures [118], while the original format of the CSCT (intersection of load-deformation relationship and failure criterion [33], which is more general) has been integrated in Annex I dedicated to a more refined assessment of existing structures.

Since Equation 4 was analytically derived from a mechanical model, the required adaptions to deal with other effects can be easily derived on a rational manner. This is for instance the case of axial or prestressing forces, whose effects can be dealt with in a suitably and straight forward manner in the frame of the CSCT by considering them in the evaluation of the strain in the reinforcement as suggested in reference [105]. Equation 2 can thus be adapted to calculate the reinforcement strain accounting for the presence of axial or prestressing forces. For example, in the case of a centered axial force, Equation 2 becomes (see Figure 9a; see also [105], [123]):

$$\varepsilon_s = \frac{V\cdot a' + N\cdot\left(z-\left(d-\frac{h}{2}\right)\right)}{z\cdot\rho\cdot b\cdot d\cdot E_s} = \frac{V}{z\cdot\rho\cdot b\cdot d\cdot E_s}\cdot\left(a' + \frac{N}{V}\cdot\left(z-d+\frac{h}{2}\right)\right) \approx \frac{V}{z\cdot\rho\cdot b\cdot d\cdot E_s}\cdot\underbrace{\left(a' + \frac{N}{V}\cdot\frac{d}{3}\right)}_{a_{cs}} \tag{5}$$

An effective shear span a_{cs} considering the effect of a centered axial force which can be used directly in Equation 4 can thus be established from an analytical (Equation 5) and a graphical manner (Figure 9) (approach valid for both compression and tension axial forces). As shown in Figure 9b, an effective shear span can also be calculated for the cases of prestressing. This approach shows that a case with an external compressive axial force acting on the compression side (Figure 9c) would not lead to an increase of the shear resistance, contradicting the provisions of current standards.

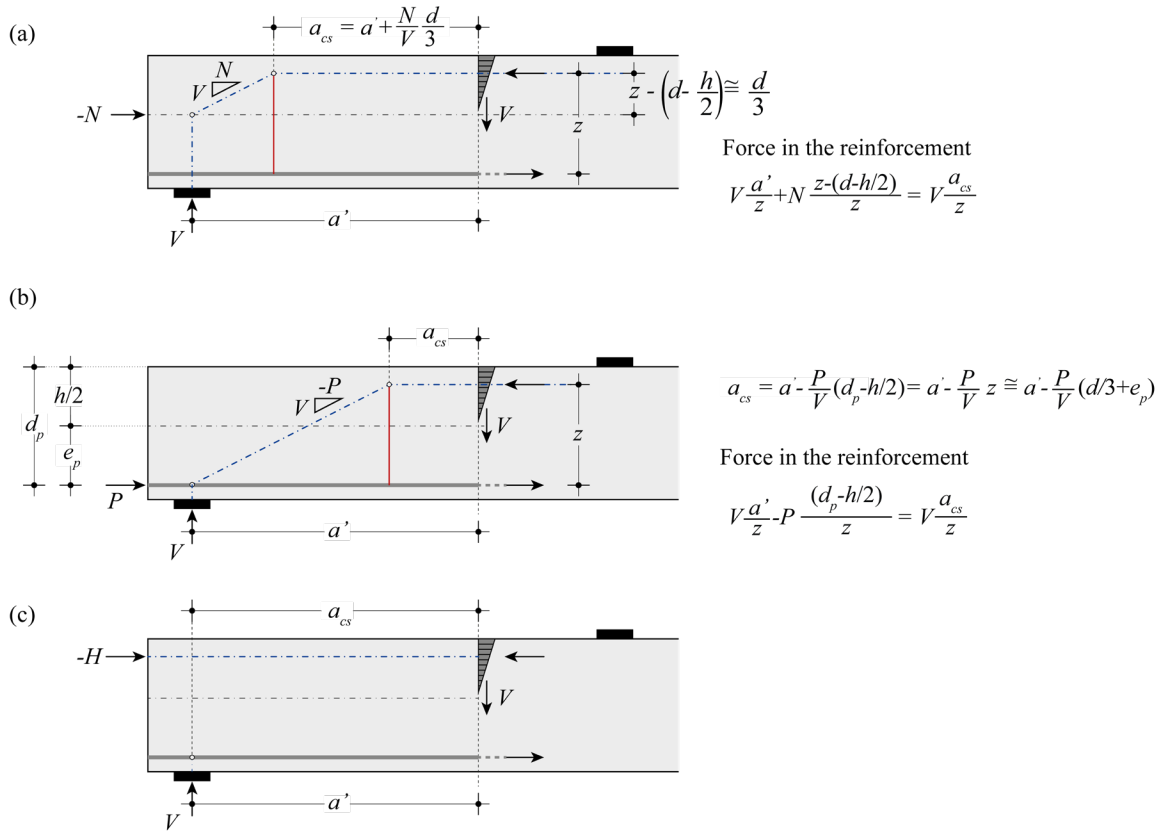

Figure 9. Considering the effects of (a) centered axial forces, (b) prestressing forces and (c) eccentric normal forces on the calculation of the effective shear span. Figure adapted from [105].

3.2 Punching shear

3.2.1 Recent experimental evidence and associated challenges

Beyond the differences between one-way shear and punching shear from a theoretical point of view, there is also an important difference from an experimental point of view. The behavior of one-way slabs without shear reinforcement is typically investigated experimentally on beams with a rectangular cross section with a limited width [99]. This allows tracking and observing the development of cracking over the depth of the members during

loading in an almost instantaneous manner (e.g. [29], [119]). In punching shear tests, with the available measuring techniques today available, it is only possible to follow the development of cracking and strains in bottom and top surfaces and attempts to follow the development of crack inside the slabs in a detailed manner are at the beginning [84]. This lack of insight information makes it difficult to fully validate some of the assumptions of a mechanical model for punching. An additional level of uncertainty with respect to shear results therefore in the interpretation of the phenomena governing the failures. Notwithstanding, a number of interesting experimental evidence are reported in literature, allowing to ground the most relevant hypotheses of a mechanical model. For that purpose, some analogies with the experimental evidence resulting from the shear tests can also be used. This is what has been done by Simões et al. [85], who combined experimental observations with the main principles of the CSCT to develop a more refined mechanical model.

3.2.2 Refined formulation of the mechanical model for punching

As previously discussed, the CSCT for punching considers that the propagation of an inclined tangential flexural crack towards the compression zone governs the capacity to transfer shear forces from the slab to the column [32], [37], [39]. The location, shape and kinematics of this crack are therefore instrumental to calculate the punching shear resistance and the associated deformation capacity [85].

Simões et al. [85] presented a refinement of the mechanical model consisting of an advanced formulation to calculate the failure criterion. Such model is grounded on experimental evidence and theoretical considerations.

The CSC is an inclined surface presenting two regions with distinct behaviors [34] (see Figure 10a): a localized cracking on the tension side and a smeared cracking on the compression side. On the localized cracking region, a crack is formed, and the transmission of forces occurs by aggregate interlocking [35], [58], [108] and residual tensile strength [124]. On the smeared cracking region, a shear band behavior is adopted (inspired on the work by Jensen [125], but adopting a strain-stress relationship for concrete [59] accounting for strain softening [3] and biaxial compression [126]), consisting on the consideration of a distributed cracking (eventually with coalescence at failure) over a given width (corresponding to the width of the band). The location of the CSC at the level of the flexural reinforcement (see the parameter r_0 in Figure 10a-10b) is governed by the formation of the outermost tangential flexural cracks. Its kinematics is composed by the vector sum of a flexural (in blue in Figure 10c) and a shear deformation (in red in Figure 10c), as originally idealized in references [28], [32], considered in [58], [60] and supported from an experimental point-of-view by the work of Clément [60]). On the basis of the calculated displacements between the two crack lips, the shear-transfer forces developing along the CSC can be evaluated based on advanced constitutive laws (see Simões et al. [85] for their description). For a given rotation and the corresponding shear deformation at maximum load, the punching resistance is obtained by summing the contributions of the different shear-transfer actions (Figure 10d). References [85], [86] can be consulted for further details.

The results of the refinement of the mechanical model of the CSCT [85] show a decreasing punching resistance with increasing rotation in accordance with previous failure criteria [32], [37], [39], which is explained by the reduction of the different shear-transfer contributions. Larger rotations mean wider cracks which [85]: (1) reduce the aggregate interlocking stresses in the localizing cracking region; (2) reduce the strength in the smeared cracking region and (3) are normally associated with yielding of radial flexural reinforcement, reducing or even disabling the contribution of dowel-action.

The calculations [70], [85] which reproduce the behavior of tests on slab and footing specimens (databases from [34]) are plotted in Figure 11a in terms of normalized punching shear resistance as a function of a normalized rotation and in Figure 11b in terms of crack opening (at a height $d/2$ from the intrados) as a function of the normalized rotation. Figure 11a shows that: (1) the calculated values fall within a band which can be approximated by a single analytical function (the hyperbolic failure criterion of reference [39] represents a good approximation of such function) [85]; (2) while the simulation of slab specimens are distributed along a wide range of normalized rotations, the results for isolated footings show that these members fail for limited values of the normalized rotation; (3) even if the calculation for the isolated footings are within the ones observed for slender slabs, it seems possible to observe a trend of a more pronounced decrease of the punching resistance with the increase of the normalized rotation for isolated footings than for slender slabs (this could be justified by the rather small values of the column size-to-effective depth ratio occurring in footings, see also Figure 12a for parametric study on the influence of the column size). Figure 11b shows that: (1) a linear correlation between the crack opening and the multiplication of the rotation by the effective depth $w_T \propto \psi \cdot d$ as originally idealized in references [32], [37], [39] to determine the bending related crack opening is a fair approximation of the calculated behavior for medium to large flexural deformations; (2) for limited flexural deformations (low rotations), the shear deformation becomes the governing contribution to the crack opening; (3) the isolated footings are mainly in this regime; (4) these results are in-line with the adoption of power-law failure

criterion [34], [87] with an upper limit corresponding to the maximum achievable punching shear resistance (again, associated to a failure mechanism rather governed by the shear deformations [34]).

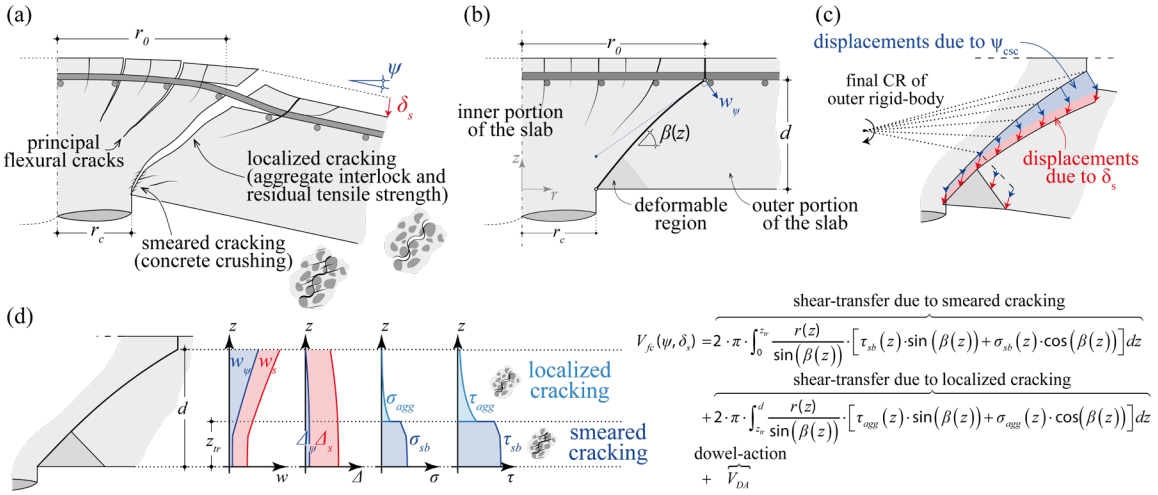

Figure 10. Mechanical model of Simões et al. [85]: (a) main assumptions; (b) different regions of the slab; (c) kinematics; (d) geometry, displacements normal and parallel to the CSC, normal and shear stresses and integration of stresses along the CSC. Figure adapted from [85], [86].

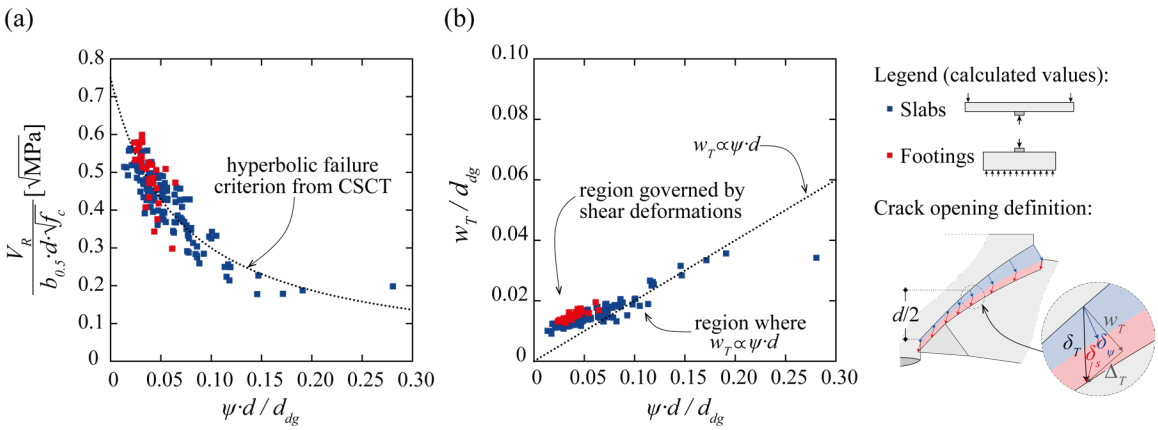

Figure 11. Results of the refined mechanical model of the CSCT for punching [85]: (a) normalized punching resistance calculated for selected tests (databases from [34]) as a function of the calculated normalized rotation; (b) calculated normalized crack opening at $d/2$ from the soffit of the slab as a function of the normalized rotation. Figure adapted from Simões et al. [85].

Another possible interesting application of the CSCT is the calculation of the shear deformation not only at failure, but also during loading. Such a deformation is for instance interesting to investigate (1) the activation of the shear reinforcement, and (2) the redistributions of the shear forces due to nonlinear shear deformation around non-axis-symmetric supports like edge and corner columns or columns with unbalanced moments.

According to the refined mechanical model presented by Simões et al. [85], the shear deformation associated to a given punching load can be calculated with the following iterative procedure: (1) assume a rotation ψ; (2) calculate the associated acting load based on the load-rotation relationship; (3) assume an initial shear deformation and increase it incrementally until the calculated shear force which can be activated across the CSC corresponds to the load of step (2). The results of such approach are for instance presented in Figure 13 for two slab specimens tested by Einpaul et al. [42] and Einpaul [127]: for the sake of comparison, the calculated vertical displacement at the root of the column (associated to the shear deformation) is compared against the maximum measured deviation from a conical shape deformation of the slab. The calculated and measured values are in excellent agreement, indicating that the refined mechanical model is not only capable of predicting the shear deformation at failure, but can also estimate the shear and flexural deformations for lower load levels. A parametric study relating the rotation-shear deformation-punching load during loading up to failure is shown in Figure 14.

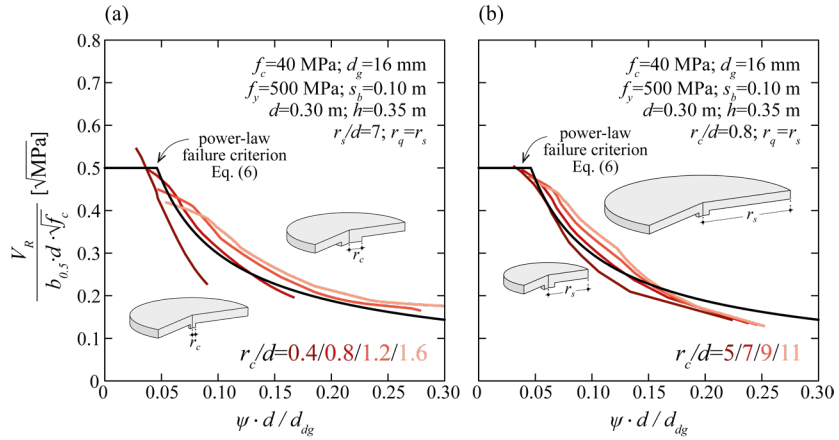

Figure 12. Normalized punching resistance as a function of the normalized rotation calculated with the refined mechanical model [85] and comparison with simplified power-law failure criterion [34], [104] for different: (a) column size-to-effective depth ratios; (b) slenderness-to-effective depth ratios. Figure adapted from [86].

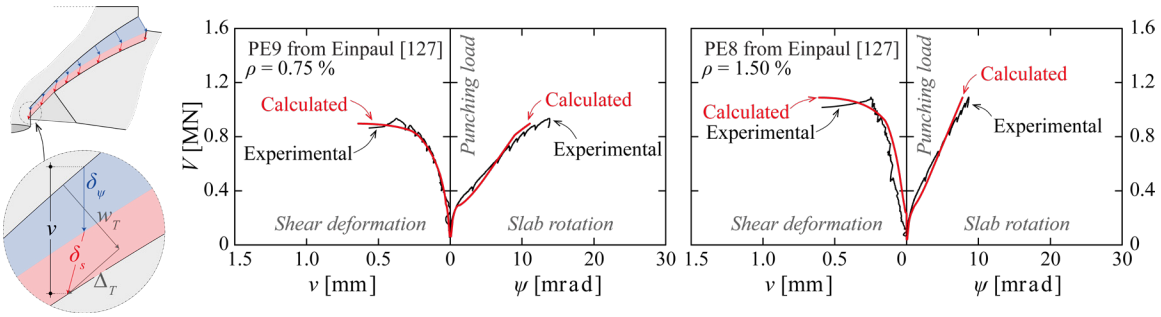

Figure 13. Comparison of the results of the refined mechanical model of the CSCT for punching [85] against experimental results (from [127]) in terms of shear and flexural deformations.

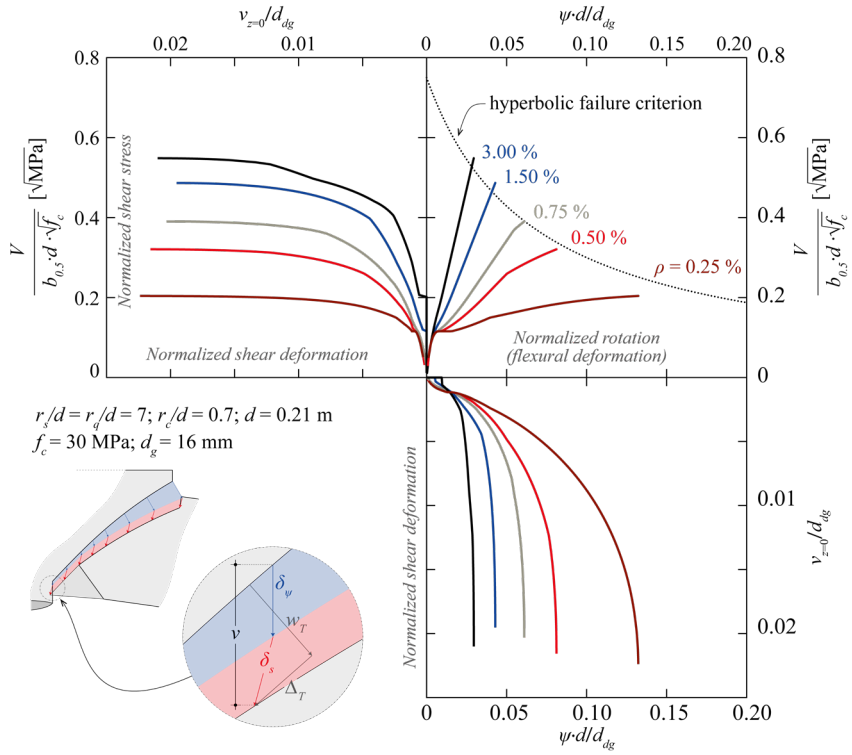

Figure 14. Results of the refined mechanical model of the CSCT for punching [85]: relationship between load, rotation and shear deformation during loading and at failure.

3.2.3 Closed-form expressions and integration to codes of practice

As discussed in Section 2, the strain-based version of the CSCT for punching shear has been integrated in codes of practice since 2003 (Swiss Code SIA 262:2003 [25], see [37], [39], [93]. From a practical point of view, the application of this theory to punching shear design or assessment has been normally performed calculating the resistance associated with the rotation calculated based on the applied design load (considering the appropriate partial safety factor and characteristics values). This methodology is simple to use for the design of new structures, as it consists on a simple comparison of a design resistance to a design load. An iterative procedure is nevertheless required to calculate the load where the design resistance equals the design load, thus corresponding to the punching resistance.

In the scope of the review of the design expressions for the punching shear provisions in the new generation of the Eurocode for reinforced concrete structures [118], one of the objectives was to improve the ease-of-use. Considering that Eurocode 2 provides in its current version an expression for the calculation of the punching resistance that, although empirical (based on Zsutty's work for shear [8]), is closed-form and relatively easy to use, a reformulation of the CSCT expressions has been seen as suitable. It thus resulted in the need to develop analytical closed-form expression for the punching shear design in the framework of the CSCT. As the hyperbolic failure criterion does not allow for the analytical derivation of such expressions, it was necessary to approximate it with a function that could allow it. A power-law failure criterion was considered to be a justified choice as follows [34], [104]:

$$\frac{V_{R,c}}{b_{0.5}\cdot d_v\cdot\sqrt{f_c}} = 0.55\cdot\left(\frac{d_{dg}}{25\cdot\psi\cdot d}\right)^{\frac{2}{3}} \leq k_F \tag{6}$$

where d_v is the shear-resisting effective depth, $b_{0.5}$ is the length of the control perimeter at a distance $0.5d_v$ for the column face (see subsection 3.2.5 below) and k_F is the upper limit of the failure criterion (maximum achievable punching shear resistance for small rotations; a value between 0.45 and 0.65 can be considered [34]) being associated to a failure mostly governed by shear deformations (refer to Figure 11b; see [34] for further discussion on this topic). Figure 12 shows a comparison between a parametric study performed with the refined mechanical model of the CSCT [85] and the power-law failure criterion of Equation 6. These results, as others previously presented [34], [85], [86], show that the consideration of an analytical power-law failure criterion is a reasonable compromise between the results of the refined mechanical model and the simplicity required for the derivation of a closed-form solution for the punching resistance of reinforced concrete members to be implemented in a standard.

The load-rotation relationship according to [39], [117] was already a power-law and has been slightly adapted with respect to the influence of a_p to better approximate the results of the refined mechanical model:

$$\psi = k_m\frac{8\cdot a_{pd}}{d}\frac{f_y}{E_s}\left(\frac{V}{V_{flex}}\right)^{3/2} \tag{7}$$

where $a_{pd} = \sqrt{a_p\cdot\frac{d}{8}}$, where a_p refers to the distance between the center of the support area and the point of contraflexure.

Based on Equations 6-7, simple expressions for punching shear design can be analytically derived (as already shown in references [34], [87], [88], [128]). For the sake of simplicity, the derivation will be quickly revisited below considering the case of interior columns, without unbalanced moment and without any column penetration (d_v=d considered in the following, i.e. an equal flexural and shear-resisting effective depth).

Introducing Equation 7 into the failure criterion of Equation 6 and solving for V=V_{Rc}, the punching shear resistance can be calculated in a closed-form format as follows [87]:

$$V_{R,c} = \sqrt{V_{flex}\cdot 0.55\cdot b_{0.5}\cdot d\cdot\sqrt{f_c}}\cdot\left(\frac{d_{dg}}{25\cdot k_m\cdot 8\cdot a_{pd}}\cdot\frac{E_s}{f_y}\right)^{\frac{1}{3}} \leq k_F\cdot b_{0.5}\cdot d\cdot\sqrt{f_c} \tag{8}$$

Equation 8 allows calculating the punching resistance without any iteration as a function of the different parameters which can be calculated on a mechanical basis (concrete type, reinforcement properties, column size, slab flexural resistance of the slab and slab slenderness). Equation 8 can further be simplified obtaining a direct function of only geometrical and mechanical parameters. For that purpose, it can be assumed that V_{flex}=$a\cdot m_R$, $m_R\approx 0.75d^2(\rho f_y)^{0.9}f_c^{0.1}$ [34], [87], E_s=200 000 MPa (applicable only for steel reinforcement), k_F=0.5 and k_m=1.2 thus eventually yielding the following expression (simplifying exponents with minor influences, refer to [34] for further details on these simplifications):

$$\frac{V_{R,c}}{b_{0.5}\cdot d} = 0.60\cdot k_{pb}\cdot\left(100\rho\cdot f_c\cdot\frac{d_{dg}}{a_{pd}}\right)^{1/3} \leq k_F\cdot\sqrt{f_c} \tag{9}$$

where the parameter $k_{pb} = \sqrt{\frac{8}{(1.2)^2} \cdot a \cdot \frac{d}{b_{0.5}}}$ (for the adopted assumptions, i.e. case without any concentration of shear forces along the control perimeter and d_v=d). Equation 9 presents a similar format as in current Eurocode 2 [118], but differs by: (a) considering a control perimeter located closer to the supporting area (see discussion in section 3.2.5 for further details); (b) considering the concrete type (by means of the factor d_{dg}); (c) including strain and size effects [67] by means of the factor $(d_{dg}/a_{pd})^{1/3}$.

In addition to the punching shear resistance, the rotation at failure (ψ_{Rc} as represented in Figure 15a) can also be calculated in a closed-form format by introducing Equation 8 into Equation 7 as follows:

$$\psi_{R,c} = \left(\frac{0.55 \cdot b_{0.5} \cdot d \cdot \sqrt{f_c}}{V_{flex}}\right)^{\frac{3}{4}} \left(\frac{k_m \cdot 8}{25} \cdot \frac{a_{pd}}{d} \frac{f_y}{E_s} \frac{d_{dg}}{d}\right)^{\frac{1}{2}} \leq k_m \frac{8 \cdot a_{pd}}{d} \frac{f_y}{E_s} \left(\frac{k_F \cdot b_{0.5} \cdot d \cdot \sqrt{f_c}}{V_{flex}}\right)^{\frac{3}{2}} \tag{10}$$

Equation 10 can be further simplified following the same considerations adopted to simplify Equation 8 to Equation 9 (considering steel reinforcement, rounding exponents and canceling parameter with minor influence), eventually yielding:

$$\psi_{R,c} = C_1 \left(\frac{a_p}{d}\right)^{1/4} (f_c)^{1/3} \left(\frac{1}{\rho}\right)^{2/3} \left(\frac{1}{k_{pb}}\right)^{3/2} \left(\frac{d_{dg}}{d}\right)^{1/2} \leq C_2 \frac{a_{pd}}{d} f_c^{3/5} \frac{1}{k_{pb}^3} \left(\frac{1}{\rho}\right)^{4/3} \tag{11}$$

where C_1 and C_2 are constants cumulating the multiplication of other constants or parameters with minor impact (parameter with exponents smaller than 0.35 are canceled). It is important to note that the left and right sides of the inequalities (Equations 10-11) refer respectively to the situation where the load-rotation relationship intersects the failure criterion in the power-law descending branch and the upper limit of the failure criterion (plateau).

For members with shear reinforcement, failure can occur by (1) crushing of the inclined concrete struts (maximum punching resistance); (2) within the shear-reinforcement zone; and (3) outside the shear-reinforced zone [44]. Other failure modes are also possible if current widely accepted detailing rules related to anchorage and spacing of the shear reinforcement are not respected. Within the framework of the CSCT, the punching resistance related to crushing of the concrete struts is normally determined by multiplying the failure criterion by an enhancement factor which depends on the type and detailing rules of the shear reinforcement [44], [49]. The punching resistance outside the shear-reinforce zone is calculated considering the corresponding control section and a reduced effective depth (function of the type of shear reinforcement) [44].

The derivation of closed-form expressions for the cases of failures due to crushing of concrete struts or outside the shear-reinforced region can be performed in a similar manner as shown above for the case of members without shear reinforcement (see [128] for further details). For failures within the shear reinforced region, the calculation of the punching resistance can be simplified as described in the following. According to reference [44], and as introduced in *fib* Model Code 2010 [116], the punching resistance in this case ($V_{R,cs}$) can be calculated considering the sum of the concrete and shear reinforcement contributions as follows (again, for an axisymmetric case, i.e. without concentration of shear forces along the control perimeter) [44]:

$$V_{R,cs} = V_{R,c,E} + V_{R,s,E} \geq A_{sw} \cdot f_{yw} \tag{12}$$

where $V_{R,c,E}$ and $V_{R,s,E}$ refer respectively to the concrete and shear reinforcement contributions at failure, which are a function of the state of deformations (described by the slab rotation ψ_E associated to the acting punching load V_E).

A relationship between the rotation ψ_E associated to the acting punching load V_E and the rotation at failure of the slab without shear reinforcement (associated to the punching resistance V_{Rc}) can be established based on the load-rotation relationship of Equation 7 as follows:

$$\frac{\psi_E}{\psi_{R,c}} = \left(\frac{V_E}{V_{R,c}}\right)^{3/2} \tag{13}$$

The concrete contribution associated to the slab rotation ψ_E can be obtained in a simplified manner using the relationship of Equation 13 together with the failure criterion of Equation 6 as (neglecting in addition the upper-limit of the failure criterion):

$$V_{R,c,E} = V_{R,c} \left(\frac{\psi_{R,c}}{\psi_E}\right)^{\frac{2}{3}} = V_{R,c} \cdot \frac{V_{R,c}}{V_E} = V_{R,c} \cdot \eta_c \tag{14}$$

where $\eta_c = V_{R,c}/V_E \leq 1$ is the analytically derived reduction factor that accounts for the decrease of the concrete contribution with the increased acting shear force allowed by the use of shear reinforcement.

With respect to the shear reinforcement contribution, it can be calculated (again, for an axisymmetric case, i.e. without concentration of shear forces along the control perimeter) multiplying the stress in the shear reinforcement (σ_{sw})

by the total area of shear reinforcement that can be activated (ΣA_{sw}; located between 0.35d and d from the column face according to [116]):

$$V_{R,s} = \sum A_{sw} \cdot \sigma_{sw} \tag{15}$$

The activable stress in the shear reinforcement in Equation 15 can be estimated based on the following expression (see [44] for further details on its derivation; second term of the left side of the inequality referring to the increase in the shear reinforcement stress due to bond; see Figure 15b for graphical representation):

$$\sigma_{sw} = \frac{E_{sw}}{6} \cdot \psi + \tau_b \cdot \frac{d}{\phi_w} \leq f_{yw} \tag{16}$$

where E_{sw} is the modulus of elasticity, τ_b is the average bond stress and ϕ_w is the diameter of the shear reinforcement bars. It should be noted that Equation 16 was derived in 2009 [44] neglecting the contribution of shear deformations to the crack opening (see line in Figure 11b), and thus to the shear reinforcement activation. This Equation provides nevertheless reasonable results when compared to the experimental tests.

Considering the relationship of Equation 13 and that $\eta_c = V_{R,c}/V_E$, the rotation ψ_E associated to the acting shear force can be written as a function of the rotation at failure of a member without shear reinforcement and the acting shear force as:

$$\psi_E = \psi_{R,c} \left(\frac{1}{\eta_c}\right)^{3/2} \tag{17}$$

The shear reinforcement stress at failure can be calculated introducing ψ_E according to Equation 17 in Equation 16:

$$\sigma_{sw} = \frac{E_{sw}}{6} \psi_{R,c} \left(\frac{1}{\eta_c}\right)^{3/2} + \tau_b \cdot \frac{d}{\phi_w} \leq f_{yw} \tag{18}$$

Equation 18 can eventually be simplified (to be a direct function of geometrical and mechanical parameters) introducing $\psi_{R,c}$ according to Equation 11 (considering in addition that the intersection with the power-law function is governing, i.e., the rotation is given by the left side of the inequality) as:

$$\sigma_{sw} = \frac{E_{sw}}{6}\ C_1 \left(\frac{a_p}{d}\right)^{1/4}\ (f_c)^{1/3} \left(\frac{1}{\rho}\right)^{2/3} \left(\frac{1}{k_{pb} \cdot \eta_c}\right)^{3/2} \left(\frac{d_{dg}}{d}\right)^{1/2} + \tau_b \cdot \frac{d}{\phi_w} \leq f_{yw} \tag{19}$$

From a practical point-of-view, the parameters (a_p/d and f_c) with the least influence on the shear reinforcement stress can be cancelled considering realistic, yet unfavorable values. The influence of the flexural reinforcement ratio can also be cancelled based on the assumption that a rather large value of this parameter is normally used in the case of members with shear reinforcement (to avoid the flexural resistance to be the governing criterion). With such reasonings, Equation 19 can eventually be simplified as follows for slabs with steel shear reinforcement (constant value of E_{sw}):

$$\sigma_{sw} = C_3 \left(\frac{1}{k_{pb} \cdot \eta_c}\right)^{3/2} \left(\frac{d_{dg}}{d}\right)^{1/2} + \tau_b \cdot \frac{d}{\phi_w} \leq f_{yw} \tag{20}$$

where C_3 is a constant absorbing the multiplication of other constant value as well as the constants resulting from the cancelling of the previously mentioned parameters.

Using Equations 14 and 20, Equation 12 can be rewritten in a simpler format as:

$$V_{R,cs} = \eta_c \cdot V_{R,c} + \eta_s \cdot \rho_{sw} \cdot b_{0.5} \cdot d \cdot f_{yw} \geq \rho_{sw} \cdot b_{0.5} \cdot d \cdot f_{yw} \tag{21}$$

where η_s is a factor accounting (1) for the activation of the shear reinforcement and (2) for the fact that a total area of shear reinforcement (ΣA_{sw}) smaller than $\rho_{sw} \cdot b_{0.5} \cdot d$ based on the principle of *fib* Model Code 2010 (where the only the units of shear reinforcement between 0.35d and d from the face of the supporting area can be activated; this consideration is slightly relaxed for the lower limit of Equation 21 [128]). This factor is calculated according to Equation 22:

$$\eta_s = \frac{\sigma_{sw}}{f_{yw}} \cdot \frac{\sum A_{sw}}{\rho_{sw} \cdot b_{0.5} \cdot d} \leq \frac{\sum A_{sw}}{\rho_{sw} \cdot b_{0.5} \cdot d} \tag{22}$$

which yields an equation of the following type:

$$\eta_s = \underbrace{\frac{C_3}{f_{yw}} \frac{\sum A_{sw}}{\rho_{sw} \cdot b_{0.5} \cdot d}}_{C_4 \cdot C_6} \left(\frac{1}{k_{pb} \cdot \eta_c}\right)^{3/2} \left(\frac{d_{dg}}{d}\right)^{1/2} + \underbrace{\frac{\tau_b}{f_{yw}} \frac{\sum A_{sw}}{\rho_{sw} \cdot b_{0.5} \cdot d}}_{C_5 \cdot C_6} \cdot \frac{d}{\phi_w} \leq \underbrace{\frac{\sum A_{sw}}{\rho_{sw} \cdot b_{0.5} \cdot d}}_{C_6} \tag{23}$$

where the values of C_4 to C_6 can be assumed to be constant without a significant loss of generality.

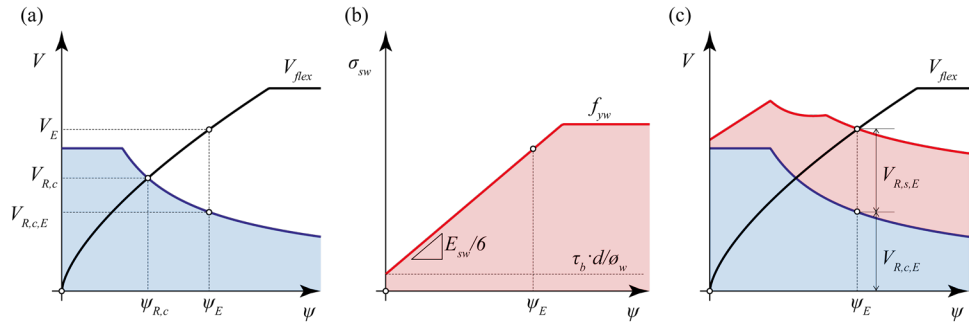

Figure 15. Graphical representation of the analytical derivation of simplified punching shear design formulae for FprEN 1992-1-1:2023 [118] based on the CSCT: (a) closed-form for members without shear reinforcement; (b) activation of shear reinforcement; (c) members with shear reinforcement.

Equations 9 and 21 (together with Equations 14 and 23), formulated in an appropriate safety format [129], are the basis for the punching shear design of the next generation of the European Standards for Concrete Structures [118]. They are derived from the mechanical model, which allows to understand the limitations that result from the process of simplification to enhance their easiness of use. Figure 16 presents for instance the principles of the application of these equations to different control sections, having as objective to reduce the required area of shear reinforcement in the outer perimeters.

The derivation of design expressions from advanced physically sound models ensures also the possibility to have simple design expressions which are consistent with higher Levels-of-Approximation [130]. This is for instance the case of Annex I of FprEN 1992-1-1:2023 [118], dedicated to a refined assessment of critical existing structures, where the application of the original rotation-based formulation of the CSCT for punching (identical to the one included in the *fib* Model Code 2010 [116]) is allowed.

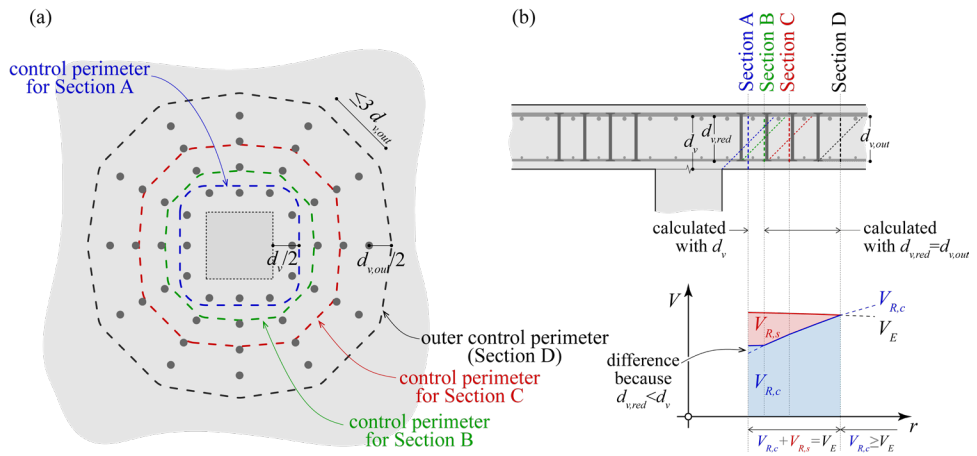

Figure 16. Investigation of the required amount of shear reinforcement by varying the location of the control section as allowed in FprEN 1992-1-1:2023 [118].

3.2.4 Considerations on the control perimeter and the actual level of the support area

Different control perimeters to verify a flat slab for punching have been adopted in standards (see Figure 17a):

- located at a distance $d/2$ from the support area as adopted by several standards (see for instance the ACI 318 [131] and the CEB-FIP Model Code 1978 [132]);
- located at a larger distance from the support area ($2d$ according to CEB-FIP Model Code 1990 [115] and EN 1992-1-1:2004 [122]).

The choice of a larger distance ($2d$) was intended to allow for an assessment of the resistance independently from the column size, but presents several drawbacks (does not represent the reality; is valid only for flat slabs without shear reinforcement and requires to be adapted for slabs with shear reinforcement and for foundations; leads to unsafe predictions for small columns requiring an additional verification nearer to the column) [128].

For the CSCT, since it is a mechanical model, the distance $d/2$, which reproduces more accurately the actual failure mechanism, has been adopted. A theoretical investigation has shown that this choice provides reasonable results for all

combinations of column sizes, slab depths and soil reactions in case of foundations. Since for larger columns, the length of the control perimeter increases, also the total punching shear resistance increases. This has a as consequence an increase of the flexural deformation ψ at failure, and thus, a decrease of the punching shear stress resistance (decreasing slope of the failure criteria, see Figures 11a and 12). This effect is explicitly accounted for in the rotation-based approach of the CSCT (and in the *fib* Model Code 2010 [116], since the rotation ψ at failure is explicitly considered), whereas in the analytical derivation of the closed-form approach implemented in the second generation of Eurocode 2 FprEN 1992-1-1:2023 [118], the same effect is accounted for with the coefficient k_{pb} in Equation 9. Interestingly, the choice of a control perimeter located at 2*d* from the column face according to EN 1992-1-1:2004 [122] provides similar results as shown in Figure 17b for circular columns. The same effect is accounted for also in ACI 318 [131], where for large columns, a strength reduction is considered based on empirical observations [133].

For large square and rectangular columns, an additional detrimental effect needs to be considered. In these cases, the slab tends to lean on the column corners and even to lift from the intermediate parts [57]. Due to the brittleness of the failure mode, only a limited redistribution of the internal forces can take place and punching can occur before significant slab shear forces can be activated at the intermediate parts. For these reasons, the length of straight segment of the control perimeter according to *fib* Model Code 2010 [116] and FprEN 1992-1-1:2023 [118] is limited to 3*d* (1.5*d* at both sides of the corners, see Figure 18a). This reduction of the length of the control perimeter (see Figure 17d) has a consequence on the punching shear resistance (see Figure 17c), although the effect is mitigated by the nonlinearity of the relationship between length of the control perimeter and punching shear resistance (see for instance coefficient k_{pb} in Equation 9).

The phenomenon of the shear force concentrations can be observed also at wall corners and wall ends. In these cases, the punching shear verification should be conducted for the force carried by the end and corner zones with the related control perimeters (Figure 18b-18c).

In some cases, the construction joint between column and slab is higher than the slab intrados (Figure 18d). Since the casted faces of the columns are usually too smooth to carry shear stresses between the column and the slab, it is reasonable to assume that the shear force in the slab must be transferred to the column at the level of the construction joint. For this reason, the punching shear verification should be conducted on the basis of the shear carrying effective depth d_v defined in Figure 18d instead of *d* [118], [25], [116].

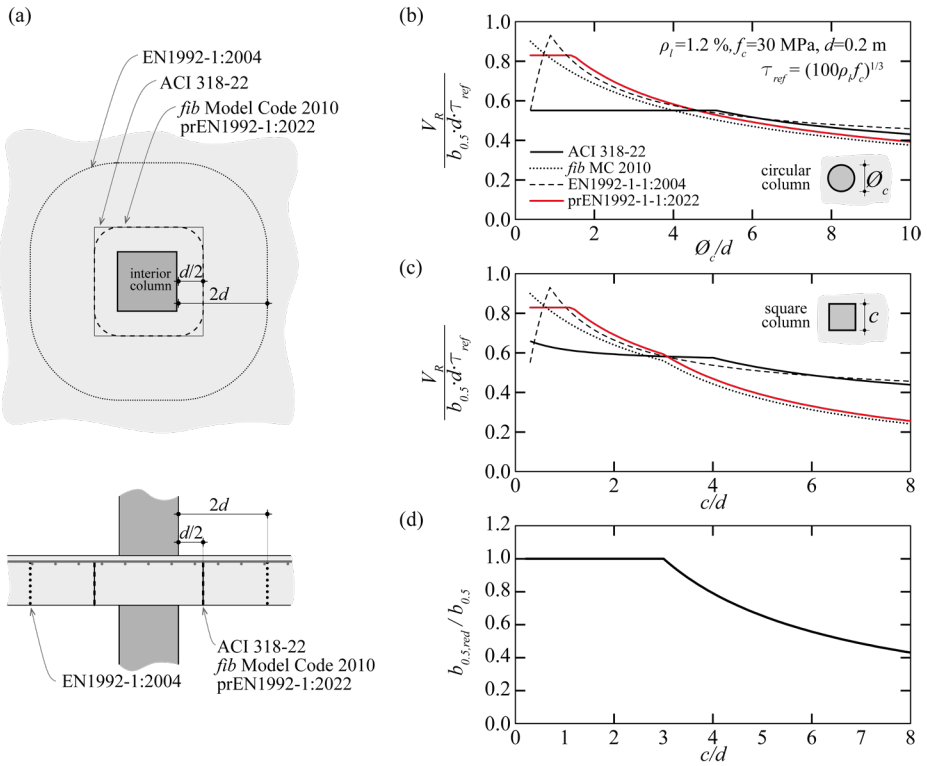

Figure 17. Considerations on the control perimeter: (a) location according to different codes of practice [122], [118], [116], [131]; influence of the column size-to-effective depth ratio on the punching resistance for (b) round and (c) square columns (accounting for stresses concentrations); (d) reduction of control perimeter in square stiff support areas due to stresses concentrations considered in [116] and [118].

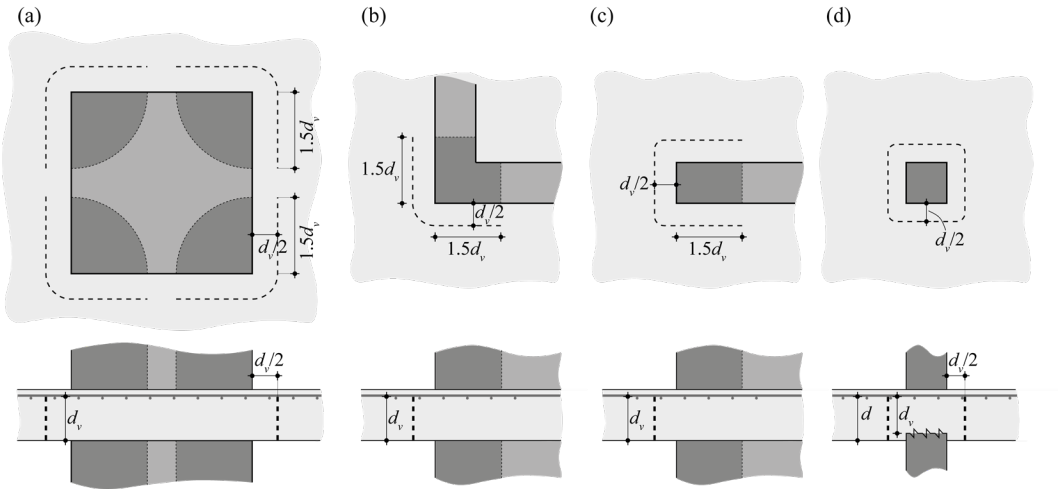

Figure 18. Definition of control perimeter according to [118]: (a) large stiff square support area; (b) corner of wall; (c) wall end; (d) interior column with column penetration.

3.2.5 Models with different levels of refinement and Levels of Approximation Approach

As shown along this document, different levels of refinement can be used in the framework of the CSCT. These different approaches are schematically presented in Figure 19, together with the indication of the cases for which the use of each of them is more interesting (see also [86] for a wider discussion on this topic).

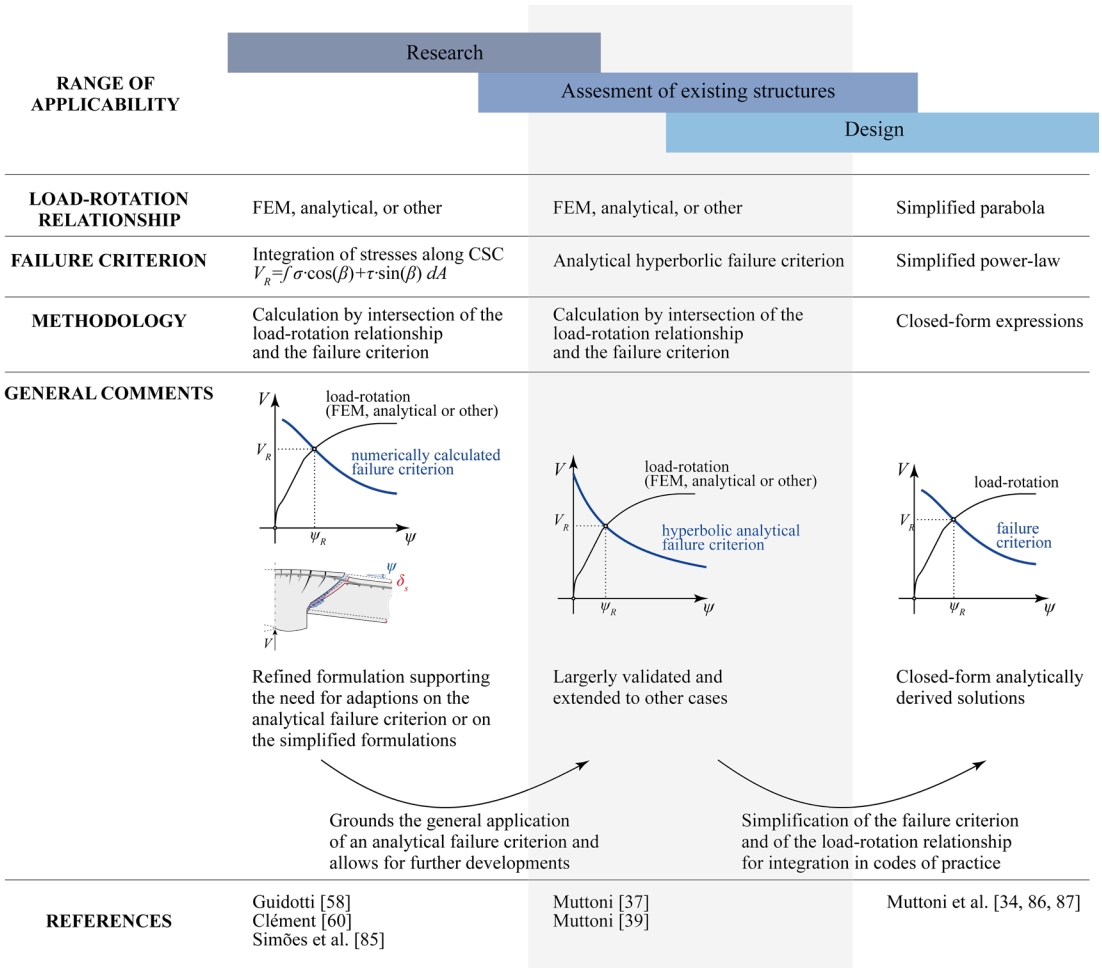

Figure 19. Overview of the framework of the mechanical model of the CSCT for punching.

4 CONCLUSIONS

This document presents a general overview of the Critical Shear Crack Theory for shear in one-way slabs without shear reinforcement and punching of slabs without and with shear reinforcement:

- The first ideas of this theory date back to 1985. Since then, the theory has strongly evolved, notably in the last 20 years. A large number of researchers from a wide range of countries from all over the world have participated in its development and validation and different research groups worldwide are using it for research purposes and to develop practical applications.
- The theory is nowadays well-established and offers the theoretical grounds for the Swiss Code for Concrete Structures since 2003, *fib* Model Code 2010 and the second generation the European standard for Concrete Structures.
- Since it is a mechanical model, it is possible to integrate it in codes via an approach based on the Levels-of-Approximation. It thus allows using closed-form expressions for simple cases, while remaining in a consistent framework which allows applying more advanced approaches for the assessment of critical existing structures and to design strengthening solutions.
- The work performed in the last years allowed the development of refined formulations for both shear and punching which can be continuously improved to incorporate new experimental evidence, new materials and new developments of construction techniques. The analytical expressions can also be easily adapted to cover new practical cases.

ACKNOWLEDGEMENTS

The first author would like to acknowledge the contributions of all the researchers who have collaborated with him in the last two decades in enhancing the Critical Shear Crack Theory.

REFERENCES

[1] A. Muttoni and M. Fernández Ruiz "Shear in slabs and beams: should they be treated in the same way?" in *fib Bulletin No. 57 – Shear and Punching Shear in RC and FRP Elements*, F. Minelli, G. Plizzari, V. Sigrist, and S. Foster, Eds., Lausanne, Switzerland: FIB, 2010, pp. 105–128.

[2] B. Thürlimann, "Plastic analysis of reinforced concrete beams," in *IABSE Colloq.: Plasticity Reinf. Concr.*, Copenhagen, Denmark, 1979, pp. 71–90.

[3] F. J. Vecchio and M. P. Collins, "The Modified Compression-Field Theory for reinforced concrete elements subjected to shear," *ACI J. Proc.*, vol. 83, no. 2, pp. 219–231, 1986.

[4] J. F. Jensen, M. P. Nielsen, M. W. Bræstrup, and F. Bach, *Some Plastic Solutions Concerning the Load-Carrying Capacity of Reinforced Concrete: Report No. R-101*. Copenhagen, Denmark: Tech. Univ. Denmark/Struct. Res. Lab., 1978 [in Danish].

[5] E. V. Bentz, F. J. Vecchio, and M. P. Collins, "Simplified modified compression field theory for calculating shear strength of reinforced concrete elements," *ACI Struct. J.*, vol. 103, no. 4, pp. 614–624, Jul./Aug. 2006.

[6] American Association of State Highway and Transportation Officials, *Bridge Design Specifications*, 9th ed. Washington, D.C., USA: AASHTO, 2020.

[7] K. G. Moody and I. M. Viest, "Shear strength of reinforced concrete beams – part 4 – analytical studies," *ACI J. Proc.*, vol. 51, no. 3, pp. 697–730, 1955.

[8] C. T. Zsutty, "Beam shear strength prediction by analysis of existing data," *ACI J. Proc.*, vol. 65, no. 11, pp. 943–951, 1968.

[9] E. Hognestad, "Shearing strength of reinforced concrete column footings," *ACI J. Proc.*, vol. 25, no. 3, pp. 189–208, 1953.

[10] R. C. Elstner and E. Hognestad, "Shearing strength of reinforced concrete slabs," *ACI Mater. J.*, vol. 53, no. 2, pp. 29–58, 1956.

[11] C. S. Whitney, "Ultimate shear strength of reinforced concrete flat slabs, footings, beams, and frame members without shear reinforcement," *ACI J. Proc.*, vol. 54, no. 10, pp. 265–298, 1957.

[12] J. Moe, *Shearing Strength of Reinforced Concrete Slabs and Footings under Concentrated Loads*. Skokie, IL, USA: Portland Cement Assoc., Res. Develop. Lab., 1961.

[13] G. N. J. Kani, "The riddle of shear failure and its solution," *ACI J. Proc.*, vol. 61, no. 4, pp. 441–468, 1964.

[14] R. C. Fenwick and T. Paulay, "Mechanisms of shear resistance of concrete beams," *J. Struct. Div.*, vol. 94, no. 10, pp. 2325–2350, 1968.

[15] H. P. J. Taylor, *Investigation of the Forces Carried Across Cracks in Reinforced Concrete Beams in Shear by Interlock of Aggregate: Technical Report N. 42*. London, UK: Cement Concr. Assoc., 1970.

[16] M. P. Nielsen, M. W. Braestrup, and F. Bach, "Rational analysis of shear in reinforced concrete beams," in *IABSE Proc.*, 1978, pp. 15–78.

[17] Y. D. Hamadi and P. E. Regan, "Behaviour in shear of beams with flexural cracks," *Mag. Concr. Res.*, vol. 32, no. 111, pp. 67–78, 1980.

[18] K.-H. Reineck, "Ultimate shear force of structural concrete members without transverse reinforcement derived from a mechanical model," *ACI Struct. J.*, vol. 88, no. 5, pp. 592–602, 1991.

[19] F. J. Vecchio, "Disturbed stress field model for reinforced concrete: formulation," *J. Struct. Eng.*, vol. 126, no. 9, pp. 1070–1077, Sep. 2000.

[20] S. Kinnunen and H. Nylander, *Punching of Concrete Slabs Without Shear Reinforcement* (Transactions of the Royal Institute of Technology 158). Stockholm, Sweden: Elan. Boktry. Aktiebol., 1960.

[21] M. W. Braestrup, M. P. Nielsen, B. C. Jensen, and F. Bach, *Axisymmetric Punching of Plain and Reinforced Concrete: Report No. 75*. Copenhagen, Denmark: Tech. Univ. Denmark, 1976.

[22] M. Hallgren "Punching shear capacity of reinforced high strength concrete slabs," Doctoral dissertation, Royal Inst. Technol., Stockholm, Sweden, 1996.

[23] D. Z. Yankelevsky and O. Leibowitz, "Punching shear in concrete slabs," *Int. J. Mech. Sci.*, vol. 41, pp. 1–15, 1999.

[24] Swiss Society of Engineers and Architects, *Code 162 for Concrete Structures*, 1993.

[25] Swiss Society of Engineers and Architects, *Code 262 for Concrete Structures*, 2003.

[26] A. Muttoni, *Punching Shear – Draft Code Proposal, SIA 162, Working Group 5*. Zürich, Switzerland: Swiss Soc. Eng. Archit., 1985.

[27] A. Muttoni and B. Thürlimann, *Shear Tests on Beams and Slabs Without Shear Reinforcement*. Zürich, Switzerland: Inst. Baustatik Konstruk., 1986.

[28] A. Muttoni, "The applicability of the theory of plasticity in the design of reinforced concrete," Doctoral dissertation, ETHZ: Zürich, Switzerland, 1990 [in German].

[29] F. Cavagnis, M. Fernández Ruiz, and A. Muttoni, "Shear failures in reinforced concrete members without transverse reinforcement: an analysis of the critical shear crack development on the basis of test results," *Eng. Struct.*, vol. 103, pp. 157–173, 2015.

[30] E. Mörsch, *The Reinforced Concrete Construction, Ist Theory and Ist Application*, 6th ed., Vol. 1.2. Stuttgart: Konrad Wittwer Ed., 1929 [in German].

[31] F. Leonhardt and R. Walther, *Shear Tests on Beams With and Without Shear Reinforcement, No. 151*. Berlin, Germany: Deut. Ausschuss Stahlbeton, 1962 [in German].

[32] A. Muttoni and J. Schwartz, "Behaviour of beams and punching in slabs without shear reinforcement," in *62 IABSE Colloq.*, Stuttgart, Germany, 1991, pp. 703–708.

[33] A. Muttoni and M. Fernández Ruiz, "Shear strength of members without transverse reinforcement as function of critical shear crack width," *ACI Struct. J.*, vol. 105, no. 2, pp. 163–172, 2008.

[34] A. Muttoni, M. Fernández Ruiz, and J. T. Simões, "The theoretical principles of the critical shear crack theory for punching shear failures and derivation of consistent closed-form design expressions," *Struct. Concr.*, vol. 19, pp. 174–190, 2018, http://dx.doi.org/10.1002/suco.201700088.

[35] J. C. Walraven, "Fundamental analysis of aggregate interlock," *J. Struct. Eng.*, vol. 107, no. 11, pp. 2245–2270, 1981.

[36] T. Frangi, D. Tonis, and A. Muttoni, "On the dimensioning od steel shear head: new finding," *Swiss Eng. Architects*, vol. 115, pp. 227–230, 1997 [in German].

[37] A. Muttoni, "Shear and punching strength of slabs without shear reinforcement," *Bet. Stahlbetonbau*, vol. 98, pp. 74–84, 2003 [in German].

[38] A. Muttoni, "Introduction to the Swiss Code SIA 262", in *Punching Shear*. Zürich, Switzerland: Swiss Eng. Archit. Document., 2003, pp. 57-66. [in French and German] [D0182].

[39] A. Muttoni, "Punching shear strength of reinforced concrete slabs without transverse reinforcement," *ACI Struct. J.*, vol. 105, no. 4, pp. 440–450, 2008.

[40] S. Guandalini, "Poinçonnement symétrique des dalles en béton armé," Ph.D. dissertation, EPFL, Lausanne, Switzerland, 2005.

[41] S. Guandalini, O. Burdet, and A. Muttoni, "Punching tests of slabs with low reinforcement ratios," *ACI Struct. J.*, vol. 106, no. 1, pp. 87–95, 2009.

[42] J. Einpaul, J. Bujnak, M. Fernández Ruiz, and A. Muttoni, "Study on influence of column size and slab slenderness on punching strength," *ACI Struct. J.*, vol. 113, no. 1, pp. 135–145, 2016.

[43] A. Torabiana, B. Isufi, D. Mostofinejada, and A. Pinho Ramos, "Behavior of thin lightly reinforced flat slabs under concentric loading," *Eng. Struct.*, vol. 196, pp. 109327, 2019, http://dx.doi.org/10.1016/j.engstruct.2019.109327.

[44] M. Fernández Ruiz and A. Muttoni, "Applications of the critical shear crack theory to punching of R/C slabs with transverse reinforcement," *ACI Struct. J.*, vol. 106, no. 4, pp. 485–494, 2009.

[45] S. Lips, "Punching of flat slabs with large amounts of shear reinforcement," Ph.D. dissertation, EPFL, Lausanne, Switzerland, 2012.

[46] S. Lips, M. Fernández Ruiz, and A. Muttoni, "Experimental investigation on punching strength and deformation capacity of shear-reinforced slabs," *ACI Struct. J.*, vol. 109, no. 6, pp. 889–900, 2012.

[47] J. Einpaul, F. Brantschen, M. Fernández Ruiz, and A. Muttoni, "Performance of punching shear reinforcement under gravity loading: influence of type and detailing," *ACI Struct. J.*, vol. 113, no. 4, pp. 827–838, 2016.

[48] R. Cantone, M. Fernández Ruiz, J. Bujnak, and A. Muttoni, "Enhancing punching strength and deformation capacity of flat slabs," *ACI Struct. J.*, vol. 116, no. 5, pp. 261–276, 2019.

[49] D. Hernández Fraile, J. T. Simões, A. Muttoni, and M. Fernández Ruiz, "A mechanical approach for the maximum punching resistance of shear-reinforced slab-column connections," in *2021 Fib Symp.*, Lisbon, Portugal, Jun. 2021, pp. 1628–1639.

[50] L. F. Maya, M. Fernández Ruiz, A. Muttoni, and S. J. Foster, "Punching shear strength of steel fibre reinforced concrete slabs," *Eng. Struct.*, vol. 40, no. 3, pp. 83–94, 2012.

[51] A. Muttoni, M. Fernández Ruiz, and J. Kunz, "Nachträgliche durchstanzbewehrung zur verstärkung von stahlbetonflachdecken," *Bauingenieur*, vol. 83, pp. 503–511. [in German].

[52] M. Fernández Ruiz, A. Muttoni, and J. Kunz, "Strengthening of flat slabs against punching shear using post-installed shear reinforcement," *ACI Struct. J.*, vol. 107, no. 4, pp. 434–442, 2010.

[53] D. M. V. Faria, J. Einpaul, A. M. P. Ramos, M. Fernández Ruiz, and A. Muttoni, "On the efficiency of flat slabs strengthening against punching using externally bonded fibre reinforced polymers," *Constr. Build. Mater.*, vol. 73, pp. 366–377, 2014.

[54] M. Lapi, A. P. Ramos, and M. Orlando, "Flat slab strengthening techniques against punching-shear," *Eng. Struct.*, vol. 180, pp. 160–180, 2019, http://dx.doi.org/10.1016/j.engstruct.2018.11.033.

[55] L. Tassinari, "Non-axissymmetric punching of flat slabs," Ph.D. dissertation, EPFL, Lausanne, Switzerland, 2011 [in French].

[56] J. Sagaseta, A. Muttoni, M. Fernández Ruiz, and L. Tassinari, "Non-axis-symmetrical punching shear around internal columns of RC slabs without transverse reinforcement," *Mag. Concr. Res.*, vol. 63, no. 6, pp. 441–457, 2011.

[57] J. Sagaseta, L. Tassinari, M. Fernández Ruiz, and A. Muttoni, "Punching of flat slabs supported on rectangular columns," *Eng. Struct.*, vol. 77, pp. 17–33, 2014.

[58] R. Guidotti, "Poinçonnement des planchers-dalles avec colonnes superposées fortement sollicitées," Ph.D. dissertation, EPFL, Lausanne, Switzerland, 2010.

[59] R. Guidotti, M. Fernández Ruiz, and A. Muttoni, "Crushing and flexural strength of slab-column joints," *Eng. Struct.*, vol. 33, no. 3, pp. 855–867, 2011.

[60] T. Clément, "Influence de la précontrainte sur la résistance au poinçonnement de dalles en béton armé," Ph.D. dissertation, EPFL, Lausanne, Switzerland, 2012.

[61] T. Clément, A. P. Ramos, M. Fernández Ruiz, and A. Muttoni, "Design for punching of prestressed concrete slabs," *Struct. Concr.*, vol. 14, pp. 157–167, 2013.

[62] T. Clément, A. P. Ramos, M. Fernández Ruiz, and A. Muttoni, "Influence of prestressing on the punching strength of post-tensionned slabs," *Eng. Struct.*, vol. 72, pp. 59–69, 2014.

[63] I.-S. Drakatos, A. Muttoni, and K. Beyer, "Internal slab-column connections under monotonic and cyclic imposed rotations," *Eng. Struct.*, vol. 123, pp. 501–516, 2016.

[64] I.-S. Drakatos, "Seismic behavior of slab-column connections without transverse reinforcement," Ph.D. dissertation, EPFL, Lausanne, Switzerland, 2016.

[65] I.-S. Drakatos, A. Muttoni, and K. Beyer, "Mechanical model for drift-induced punching of slab-column connections without transverse reinforcement," *ACI Struct. J.*, vol. 115, no. 2, pp. 463–474, 2018.

[66] A. Muttoni et al., "Deformation capacity evaluation for flat slab seismic design," *Bull. Earthq. Eng.*, vol. 20, pp. 1619–1654, 2022.

[67] M. Fernández Ruiz and A. Muttoni, "Size effect in shear and punching shear failures of concrete members without transverse reinforcement: differences between statically determinate members and redundant structures," *Struct. Concr.*, vol. 19, no. 1, pp. 65–75, 2018, http://dx.doi.org/10.1002/suco.201700059.

[68] J. T. Simões, D. M. V. Faria, M. Fernández Ruiz, and A. Muttoni, "Strength of reinforced concrete footings without transverse reinforcement according to limit analysis," *Eng. Struct.*, vol. 112, pp. 146–161, 2016.

[69] J. T. Simões, J. Bujnak, M. Fernández Ruiz, and A. Muttoni, "Punching shear tests on compact footings with uniform soil pressure," *Struct. Concr.*, vol. 17, no. 4, pp. 603–617, 2016.

[70] J. T. Simões, "The mechanics of punching in reinforced concrete slabs and footings without shear reinforcement," Ph.D. dissertation, EPFL, Lausanne, Switzerland, 2018.

[71] M. Fernández Ruiz, Y. Mirzaei, and A. Muttoni, "Post-punching behavior of flat slabs," *ACI Struct. J.*, vol. 110, pp. 801–812, 2013.

[72] J. Einpaul, M. Fernández Ruiz, and A. Muttoni, "Influence of moment redistribution and compressive membrane action on punching strength of flat slabs," *Eng. Struct.*, vol. 86, pp. 43–57, 2015.

[73] J. Einpaul, C. E. Ospina, M. Fernández Ruiz, and A. Muttoni, "Punching shear capacity of continuous slabs," *ACI Struct. J.*, vol. 113, no. 4, pp. 861–872, 2016.

[74] B. Belletti, M. Pimentel, M. Scolari, and J. C. Walraven, "Safety assessment of punching shear failure according to the level of approximation approach," *Struct. Concr.*, vol. 46, pp. 366–380, 2015.

[75] J. Shu, B. Belletti, A. Muttoni, M. Scolari, and M. Plos, "Internal force distribution in RC slabs subjected to punching shear," *Eng. Struct.*, vol. 153, pp. 766–781, 2017.

[76] B. Belletti, A. Muttoni, S. Ravasini, and F. Vecchi, "Parametric analysis on punching shear resistance of reinforced-concrete continuous slabs," *Mag. Concr. Res.*, vol. 71, no. 20, pp. 1083–1096, 2019.

[77] B. Belletti, J. C. Walraven, and F. Trapani, "Evaluation of compressive membrane action effects on punching shear resistance of reinforced concrete slabs," *Eng. Struct.*, vol. 95, pp. 25–39, 2015.

[78] D. Abu-Salma, R. L. Vollum, and L. Macorini, "Design of biaxially loaded external slab column connections," *Eng. Struct.*, vol. 249, pp. 113326, 2021, http://dx.doi.org/10.1016/j.engstruct.2021.113326.

[79] D. Abu-Salma, R. L. Vollum, and L. Macorini, "Modelling punching shear failure at edge slab-column connections by means of nonlinear joint elements," *Structures*, vol. 34, pp. 630–652, 2021.

[80] A. Setiawan, R. L. Vollum, L. Macorini, and B. A. Izzuddin, "Efficient 3D modelling of punching shear failure at slab-column connections by means of nonlinear joint elements," *Eng. Struct.*, vol. 197, pp. 109372, 2019, http://dx.doi.org/10.1016/j.engstruct.2019.109372.

[81] A. Setiawan, R. L. Vollum, L. Macorini, and B. A. Izzuddin, "Numerical modelling of punching shear failure of reinforced concrete flat slabs with shear reinforcement," *Mag. Concr. Res.*, vol. 73, no. 23, pp. 1205–1224, 2021.

[82] K. Micallef, J. Sagaseta, M. Fernández Ruiz, and A. Muttoni, "Assessing punching shear failure in reinforced concrete flat slabs subjected to localised impact loading," *Int. J. Impact Eng.*, vol. 71, pp. 17–33, 2014.

[83] J. Sagaseta, P. Olmati, K. Micalled, and D. Cormie, "Punching shear failure in blast-loaded RC slabs and panels," *Eng. Struct.*, vol. 147, pp. 177–194, 2017.

[84] J. Einpaul, M. Fernández Ruiz, and A. Muttoni, "Measurements of internal cracking in punching test slabs without shear reinforcement," *Mag. Concr. Res.*, vol. 70, no. 15, pp. 798–810, 2018.

[85] J. T. Simões, M. Fernández Ruiz, and A. Muttoni, "Validation of the Critical Shear Crack Theory for punching of slabs without transverse reinforcement by means of a refined mechanical model," *Struct. Concr.*, vol. 19, pp. 191–216, 2018, http://dx.doi.org/10.1002/suco.201700280.

[86] A. Muttoni, M. Fernández Ruiz, and J. T. Simões, "Recent improvements of the critical shear crack theory for punching shear design and its simplification for code provisions," in *Proc. 2018 Fib Congr.: Better, Smarter, Stronger*, 2019, pp. 116–129.

[87] A. Muttoni and M. Fernández Ruiz, "The Critical Shear Crack Theory for punching design: from a Mechanical Model to Closed-Form Design Expressions," in *ACI-Fib Int. Symp.: Punching Shear Test Of Structural Concrete Slabs: Honoring Neil M. Hawkins*, 2017, pp. 237–252.

[88] A. Muttoni, J. T. Simões, D. M. V. Faria, and M. Fernández Ruiz, "A mechanical approach for the punching shear provisions in the second generation of Eurocode 2," *Hormig. Acero.*, 2023, In press, http://dx.doi.org/10.33586/hya.2022.3091.

[89] J. B. Santos, A. Muttoni, and G. S. Melo, "Enhancement of the punching shear verification of slabs with openings," *Struct. Concr.*, pp. 1–18, 2022, In press, http://dx.doi.org/10.1002/suco.202200714.

[90] S. Ravasini, F. Vecchi, B. Belletti, and A. Muttoni, "Verification of deflections and cracking of RC flat slabs with numerical and analytical approaches," *Eng. Struct.*, 2023, In press.

[91] K. Qian, J.-S. Li, T. Huang, Y.-H. Weng, and X.-F. Deng, "Punching shear strength of corroded reinforced concrete slab-column connections," *J. Build. Eng.*, vol. 45, pp. 103489, 2022.

[92] M. Gołdyn and T. Urban, "UHPFRC hidden capitals as an alternative method for increasing punching of LWAC flat slabs," *Eng. Struct.*, vol. 271, pp. 114906, 2022, http://dx.doi.org/10.1016/j.engstruct.2022.114906.

[93] A. Muttoni, "Shear in Members Without Shear Reinforcement", in *Introduction to the Swiss Code SIA 262*, Zürich, Switzerland: Swiss Eng. Archit. Document., 2003, pp. 47-55.[in French and German] [D0182].

[94] M. Fernández Ruiz, A. Muttoni, and J. Sagaseta, "Shear strength of concrete members without transverse reinforcement: a mechanical approach to consistently account for size and strain effects," *Eng. Struct.*, vol. 99, pp. 360–372, 2015.

[95] R. Vaz Rodrigues, "Shear strength of reinforced concrete bridge deck slabs," Ph.D. dissertation, EPFL, Lausanne, Switzerland, 2007.

[96] R. Vaz Rodrigues, A. Muttoni, and M. Fernández Ruiz, "Influence of shear on rotation capacity of reinforced concrete members without shear reinforcement," *ACI Struct. J.*, vol. 107, no. 5, pp. 516–525, 2010.

[97] R. Vaz Rodrigues, M. Fernández Ruiz, and A. Muttoni, "Shear strength of R/C bridge cantilever slabs," *Eng. Struct.*, vol. 30, pp. 3024–3033, 2008.

[98] F. Natário, M. Fernández Ruiz, and A. Muttoni, "Shear strength of RC slabs under concentrated loads near clamped linear supports," *Eng. Struct.*, vol. 76, pp. 10–23, 2014.

[99] R. Cantone, M. Fernández Ruiz, and A. Muttoni, "Shear force redistributions and resistance of slabs and wide beams," *Struct. Concr.*, vol. 22, no. 4, pp. 2443–2465, 2021.

[100] S. Campana, M. Fernández Ruiz, A. Anastasi, and A. Muttoni, "Analysis of shear-transfer actions on one-way RC members based on measured cracking pattern and failure kinematics," *Mag. Concr. Res.*, vol. 65, no. 6, pp. 386–404, 2013.

[101] F. Cavagnis, M. Fernández Ruiz, and A. Muttoni, "An analysis of the shear transfer actions in reinforced concrete members without transverse reinforcement based on refined experimental measurements," *Struct. Concr.*, vol. 19, pp. 49–64, 2018.

[102] F. Cavagnis, J. T. Simões, M. Fernández Ruiz, and A. Muttoni, "Shear strength of members without transverse reinforcement based on development of critical shear crack," *ACI Struct. J.*, vol. 117, no. 1, pp. 103–118, 2020.

[103] F. Cavagnis, "Shear in reinforced concrete without transverse reinforcement: from refined experimental measurements to mechanical models," Doctoral dissertation, EPFL, Lausanne, Switzerland, 2017.

[104] A. Muttoni, M. Fernández Ruiz, and F. Cavagnis, "Shear in members without transverse reinforcement: from detailed test observations to a mechanical model and simple expressions for codes of practice," in *fib Bulletin No. 85: Towards a Rational Understanding of Shear in Beams and Slabs*, International Federation for Structural Concrete, Ed., Lausanne, Switzerland: FIB, 2018, pp. 7–23.

[105] A. Muttoni, M. Fernández Ruiz, and F. Cavagnis, "Shear in members without transverse reinforcement: from detailed test observations to a mechanical model and simple expressions for codes of practice," in *Fib Int. Workshop on Beam Shear*, Zurich, Switzerland, Sep. 5-6 2016.

[106] A. Muttoni and M. Fernández Ruiz, "From experimental evidence to mechanical modeling and design expressions: The Critical Shear Crack Theory for shear design," *Struct. Concr.*, vol. 20, no. 4, pp. 1464–1480, 2019, http://dx.doi.org/10.1002/suco.201900193.

[107] A. Pérez Caldentey, P. Padilla, A. Muttoni, and M. Fernández Ruiz, "Effect of load distribution and variable depth on shear resistance of slender beams without stirrups," *ACI Struct. J.*, vol. 109, no. 5, pp. 595–603, 2012.

[108] F. Cavagnis, M. Fernández Ruiz, and A. Muttoni, "A mechanical model for failures in shear of members without transverse reinforcement based on development of a critical shear crack," *Eng. Struct.*, vol. 157, pp. 300–315, 2018.

[109] C. R. Ribas González and M. Fernández Ruiz, "Influence of flanges on the shear-carrying capacity of reinforced concrete beams without web reinforcement," *Struct. Concr.*, vol. 18, no. 5, pp. 720–732, 2017.

[110] S. Campana, M. Fernández Ruiz, and A. Muttoni, "Shear strength of arch-shaped members without transverse reinforcement," *ACI Struct. J.*, vol. 111, no. 3, pp. 573–582, 2014.

[111] F. Natário, M. Fernández Ruiz, and A. Muttoni, "Experimental investigation on fatigue of concrete cantilever bridge deck slabs subjected to concentrated loads," *Eng. Struct.*, vol. 89, pp. 191–203, 2015.

[112] M. Fernández Ruiz, C. Zanuy, F. Natário, J.-M. Gallego, and A. Muttoni, "Influence of fatigue loading in shear failures of reinforced concrete members without transverse reinforcement," *J. Adv. Concr. Technol.*, vol. 13, pp. 263–274, 2015.

[113] R. Cantone, A. Setiawan, M. Fernández Ruiz, and A. Muttoni, "Characterization of shear deformations in reinforced concrete members without shear reinforcement," *Eng. Struct.*, vol. 257, pp. 113910, 2022.

[114] Swiss Society of Engineers and Architects, *Code 162 for Concrete Structures*, 1989.

[115] Comité Euro-International du Béton, *CEB-FIP Model Code 1990*, 1993.

[116] International Federation for Structural Concrete, *fib Model Code for Concrete Structures 2010*. Berlin, Germany: Ernst & Sohn, 2013.

[117] A. Muttoni, M. Fernández Ruiz, E. Bentz, S. J. Foster, and V. Sigrist, "Background to the Model Code 2010 Shear Provisions - Part II Punching Shear," *Struct. Concr.*, vol. 14, no. 3, pp. 195–203, 2013.

[118] European Committee for Standardization, *Eurocode 2 - Design of Concrete Structures - Part 1-1: General Rules - Rules for Buildings, Bridges and Civil Engineering Structures*, Final Draft FprEN 1992-1-1:2023, 2023.

[119] P. Huber, T. Huber, and J. Kollegger, "Investigation of the shear behavior of RC beams on the basis of measured crack kinematics," *Eng. Struct.*, vol. 113, pp. 41–58, 2016.

[120] M. P. Collins and D. Kuchma, "How safe are our large, lightly reinforced concrete beams, slabs, and footings," *ACI Struct. J.*, vol. 96, pp. 482–490, 1999.

[121] E. G. Sherwood, E. C. Bentz, and M. P. Collins, "Effect of aggregate size on beam-shear strength of thick slabs," *ACI Struct. J.*, vol. 104, pp. 180–190, 2007.

[122] European Committee for Standardization, *Eurocode 2. Design of Concrete Structures - Part 1-1: General Rules and Rules for Buildings*, EN 1992-1-1:2004, 2004.

[123] A. Muttoni, M. Fernández Ruiz, F. Cavagnis, and J. T. Simões, "Shear in members without shear reinforcement," in *Background Document To Fpren 1992-1-1:2023-04 (Formal-Vote-Draft*, CEN/TC 250/SC 2: Eurocode 2: Design of Concrete Structures, Ed., Italy, Eurocode, 2021, pp. 1–17.

[124] D. A. Hordijk, "Tensile and tensile fatigue behaviour of concrete, experiments, modelling and analyses," *Heron*, vol. 37, no. 1, pp. 3–79, 1992.

[125] B. C. Jensen, "Lines of discontinuity for displacements in the theory of plasticity of plain and reinforced concrete," *Mag. Concr. Res.*, vol. 2, no. 2, pp. 143–150, 1975.

[126] H. Kupfer, K. H. Hubert, and H. Rusch, "Behavior of concrete under biaxial stresses," *ACI J. Proc.*, vol. 66, no. 52, pp. 656–666, 1969.

[127] J. Einpaul, “Punching strength of continuous flat slabs,” Ph.D. dissertation, EPFL, Lausanne, Switzerland, 2016.

[128] A. Muttoni et al., “Punching,” in *Background document to FprEN 1992-1-1:2023-04 (Formal-Vote-Draft)*, CEN/TC 250/SC 2: Eurocode 2: Design of Concrete Structures, Ed., Italy, Eurocode, 2023, pp. 338–357.

[129] A. Muttoni and Q. Yu, “Partial safety factor for strain-based formulae,” in *Fib TG3.1*, Oslo, Norway, Jun. 2022, pp. 1–12.

[130] A. Muttoni and M. Fernández Ruiz, “Levels-of-approximation approach in codes of practice,” *Struct. Eng. Int.*, vol. 22, no. 2, pp. 190–194, 2012.

[131] American Concrete Institute Committee, *Building Code Requirements for Structural Concrete and Commentary*, ACI Code 318-19 (22) (Reapproved 2022), 2022.

[132] Comité Euro-International du Béton, *CEB-FIP Model Code for Concrete Structures*, 1978.

[133] M. Vanderbilt, “Shear strength of continuous plates,” *J. Struct. Div.*, vol. 8, no. 5, pp. 961–973, 1972.

Author contributions: AM: conceptualization, writing; JTS: conceptualization, writing.

Editors: Leandro Trautwein, Mauro Real, Mario Pimentel.